Geosci. Model Dev., 18, 5487–5512, 2025
https://doi.org/10.5194/gmd-18-5487-2025

Geoscientific Model Development
Open Access
EGU

Hunga Tonga–Hunga Ha'apai Volcano Impact Model Observation Comparison (HTHH-MOC) project: experiment protocol and model descriptions

Yunqian Zhu[1,2], Hideharu Akiyoshi[3], Valentina Aquila[4], Elizabeth Asher[1,5], Ewa M. Bednarz[1,2], Slimane Bekki[6], Christoph Brühl[7], Amy H. Butler[2], Parker Case[8], Simon Chabrillat[9], Gabriel Chiodo[10,11], Margot Clyne[12,13], Peter R. Colarco[8,39], Sandip Dhomse[19,20], Lola Falletti[6], Eric Fleming[8,14], Ben Johnson[40], Andrin Jörimann[10,11,38], Mahesh Kovilakam[16], Gerbrand Koren[17], Ales Kuchar[18], Nicolas Lebas[15], Qing Liang[8], Cheng-Cheng Liu[13], Graham Mann[19,20], Michael Manyin[8,14], Marion Marchand[6], Olaf Morgenstern[21,22,a], Paul Newman[8], Luke D. Oman[8], Freja F. Østerstrøm[23,24,b], Yifeng Peng[25], David Plummer[26], Ilaria Quaglia[27], William Randel[27], Samuel Rémy[28], Takashi Sekiya[29], Stephen Steenrod[8,30], Timofei Sukhodolov[38], Simone Tilmes[27], Kostas Tsigaridis[31,32], Rei Ueyama[33], Daniele Visioni[34], Xinyue Wang[12], Shingo Watanabe[29,41], Yousuke Yamashita[3], Pengfei Yu[35], Wandi Yu[36], Jun Zhang[27], and Zhihong Zhuo[37]

[1]Cooperative Institute for Research in Environmental Sciences (CIRES), University of Colorado Boulder, Boulder, CO, USA
[2]NOAA Chemical Sciences Laboratory, Boulder, CO, USA
[3]National Institute for Environmental Studies, Tsukuba, Japan
[4]American University, Department of Environmental Science, Washington, DC, USA
[5]NOAA Global Monitoring Laboratory, Boulder, CO, USA
[6]LATMOS, UVSQ, CNRS, INU, Sorbonne Université, Paris, France
[7]Max Planck Institute for Chemistry, Mainz, Germany
[8]NASA Goddard Space Flight Center, Greenbelt, MD, USA
[9]Royal Belgian Institute for Space Aeronomy (BIRA-IASB), Brussels, Belgium
[10]Institute for Atmospheric and Climate Science, ETH Zurich, Zurich, Switzerland
[11]Instituto de Geociencias, Spanish National Research Council (IGEO-CSIC-UCM), Madrid, Spain
[12]Department of Atmospheric and Oceanic Sciences, University of Colorado Boulder, Boulder, CO, USA
[13]Laboratory for Atmospheric and Space Physics, University of Colorado Boulder, Boulder, CO, USA
[14]Science Systems and Applications, Inc., Lanham, MD, USA
[15]LOCEAN/IPSL, Sorbonne Université, CNRS, IRD, MNHN, Paris, France
[16]NASA Langley Research Center, Hampton, VA, USA
[17]Copernicus Institute of Sustainable Development, Utrecht University, Utrecht, the Netherlands
[18]Institute of Meteorology and Climatology, BOKU University, Vienna, Austria
[19]School of Earth and Environment, University of Leeds, Leeds, UK
[20]UK National Centre for Atmospheric Science, University of Leeds, Leeds, UK
[21]National Institute of Water and Atmospheric Research (NIWA), Te Whanganui-a-Tara / Wellington, Aotearoa / New Zealand
[22]School of Physical and Chemical Sciences, University of Canterbury, Ōtautahi / Christchurch, Aotearoa / New Zealand
[23]School of Engineering and Applied Sciences, Harvard University, Cambridge, MA, USA
[24]Department of Chemistry, University of Copenhagen, Copenhagen, Denmark
[25]School of Atmospheric Sciences, Lanzhou University, Lanzhou, China
[26]Climate Research Division, Environment and Climate Change Canada, Montréal, Canada
[27]NCAR ACOM, Boulder, CO, USA
[28]HYGEOS, Lille, France
[29]Japan Agency for Marine-Earth Science and Technology (JAMSTEC), Yokohama, Japan
[30]GESTAR II, University of Maryland-Baltimore County, Baltimore, MD, USA

Published by Copernicus Publications on behalf of the European Geosciences Union.

[31]Center for Climate Systems Research, Columbia University, New York, NY, USA
[32]NASA Goddard Institute for Space Studies, New York, NY, USA
[33]NASA Ames Research Center, Moffett Field, CA, USA
[34]Department of Earth and Atmospheric Sciences, Cornell University, Ithaca, NY, USA
[35]Institute of environmental and climate research, Jinan University, Guangzhou, China
[36]Lawrence Livermore National Laboratory, Livermore, CA, USA
[37]Department of Earth and Atmospheric Sciences, University of Quebec in Montreal, Montreal (Quebec), Canada
[38]Physikalisch-Meteorologisches Observatorium Davos and World Radiation Center, Davos, Switzerland
[39]Earth System Science Interdisciplinary Center, University of Maryland, College Park, MD, USA
[40]Met Office Hadley Centre, Exeter, UK
[41]Advanced Institute for Marine Ecosystem Change (WPI-AIMEC), Tohoku University, Sendai, Japan
[a]now at: German Meteorological Service (DWD), Offenbach, Germany
[b]now at: Department of Environmental Science, Aarhus University, Roskilde, Denmark

Correspondence: Yunqian Zhu (yunqian.zhu@colorado.edu)

Received: 2 November 2024 – Discussion started: 18 November 2024
Revised: 1 March 2025 – Accepted: 6 June 2025 – Published: 1 September 2025

Abstract. The 2022 Hunga volcanic eruption injected a significant amount of water vapor and a moderate amount of sulfur dioxide into the stratosphere, causing observable responses in the climate system. We have developed a model–observation comparison project to investigate the evolution of volcanic water and aerosols and their impacts on atmospheric dynamics, chemistry, and climate, using several state-of-the-art chemistry climate models. The project goals are (1) to evaluate the current chemistry–climate models to quantify their performance in comparison to observations and (2) to understand atmospheric responses in the Earth system after this exceptional event and investigate the potential impacts in the projected future. To achieve these goals, we designed specific experiments for direct comparisons to observations, for example from balloons and the Microwave Limb Sounder satellite instrument. Experiment 1 consists of two sets of free-running ensemble experiments from 2022 to 2031: one with fixed sea-surface temperatures and sea ice and one with coupled ocean. These experiments will help to understand the long-term evolution of water vapor and aerosols; quantify HTHH effects on stratospheric and mesospheric temperatures, dynamics, and transport; understand the impact of dynamic changes on ozone chemistry; quantify the net radiative forcings; and evaluate any surface climate impact. Experiment 2 is a nudged-run experiment from 2022 to 2023 using observed meteorology. To allow participation of more climate models with varying complexities of aerosol simulation, we include two sets of simulations in Experiment 2: Experiment 2a is designed for models with internally generated aerosol, while Experiment 2b is designed for models using prescribed aerosol surface area density. This experiment will help to analyze H_2O and aerosol evolution, quantify the net radiative forcings, understand the impacts on mid-latitude and polar O_3 chemistry, and allow close comparisons with observations.

1 Introduction and motivations of this project

The Hunga Tonga–Hunga Ha'apai (HTHH) Impacts activity was established in the World Climate Research Programme (WCRP) Atmosphere Processes And their Role in Climate (APARC) as a limited-term focused cross-activity with a duration of 3 years. It aims to assess the impacts of the 15 January 2022 Hunga volcanic eruption and produce an assessment to document the Hunga impact on the climate system. The Hunga eruption injected an unprecedented amount of water (H_2O) and moderate sulfur dioxide (SO_2) into the stratosphere (Millán et al., 2022), presenting a unique opportunity to understand the impacts on the stratosphere of a large-magnitude explosive phreatomagmatic eruption. The wide range of satellite observations of the stratospheric water and sulfate plumes, global transport and dispersion of volcanic materials, and unusual chemical and temperature signals are helpful in assessing model representations of stratospheric chemistry, aerosol, and dynamics. For example, the Aura Microwave Limb Sounder (MLS) observed ~ 150 Tg of water injected by the Hunga eruption (Millán et al., 2022), which slowly decayed due to the polar stratospheric cloud (PSC) dehydration process and stratosphere–troposphere exchange (Fleming et al., 2024; Zhou et al., 2024). Large aerosol optical depth is observed by the Ozone Mapping and Profiler Suite (OMPS) (Taha et al., 2022), due to fast formation of sulfate (Zhu et al., 2022) and the high optical efficiency of Hunga aerosol particles (Li et al., 2024). Unlike the stratospheric warming patterns observed from previous

large volcanic eruptions (El Chichón in 1982 and Pinatubo in 1991), global stratospheric temperatures decreased by 0.5 to 1.0 K in the first 2 years following the Hunga eruption, largely due to radiative cooling from injected water vapor (Randel et al., 2024). Satellite observations in June, July, and August 2022 reveal reduced lower-stratospheric ozone (O_3) over the Southern Hemisphere (SH) midlatitudes and subtropics, with high levels near the Equator, exceeding previous variability. These ozone anomalies coincide with a weakening of the Brewer–Dobson circulation during this period (Wang et al., 2023). Changes in stratospheric winds also influence the mesosphere, leading to a stronger mesospheric circulation and corresponding temperature changes (Yu et al., 2023). These observed phenomena provide a unique opportunity to test the ability of chemistry–climate models to simulate the evolution of volcanic aerosols combined with such a large amount of water vapor, as well as understand how volcanic water vapor and aerosols modify radiative balances and stratospheric ozone.

The APARC Hunga Impacts activity aims to provide a benchmark analysis of the eruption impacts so far and projections of eruption climate impacts over the next few years. Two multi-model evaluation projects are designed to facilitate the success of this activity: the Tonga Model Intercomparison Project (Tonga-MIP) (Clyne, 2024) and the Hunga Tonga–Hunga Ha'apai Volcano Impact Model Observation Comparison (HTHH-MOC) project (this paper). The HTHH-MOC provides a foundation for a coordinated multi-model evaluation of global chemistry–climate models' performance in response to the Hunga volcanic eruption. It defines a set of perturbation experiments, where volcanic forcings – injected water vapor and aerosol concentrations – are consistently applied across participating model members. HTHH-MOC aims to assess how reliably global chemistry–climate models simulate the climate responses to this unprecedented volcanic forcing. This project enhances our confidence in attributing and interpreting observations following the Hunga eruption. The scientific questions related to the HTHH-MOC are as follows:

- How does the Hunga volcanic plumes' transport relate to or impact stratospheric dynamics (such as Brewer–Dobson circulation, polar vortex, and the quasi-biennial oscillation) and the upper atmosphere?
- What are the chemical impacts of the Hunga eruption in the stratosphere and mesosphere?
- What and how long is the radiative effect of the Hunga eruption?
- Does Hunga impact the tropospheric/surface climate?

Therefore, the HTHH-MOC project is focused on evaluating global chemistry–climate models regarding the following three science themes: (1) plume evolution, dispersion, and large-scale transport; (2) impacts on stratospheric chemistry and the ozone layer; and (3) radiative effect from the eruption and surface climate impacts. Besides the HTHH-MOC project, the assessment also includes analysis of observations and models that are not global climate models. In the following paragraph, we describe the HTHH-MOC experiment design and participating models.

2 Experiment design

There are two experiments (Exp1 and Exp2 detailed below) designed to fulfill the scientific goals. Each experiment includes a set of simulations with different volcanic injections (i.e., with and without water and/or SO_2 injections), to explore the separate impacts of volcanic water and aerosols during the post-eruption period: (a) control case (no eruption), (b) H_2O ($\sim$ 150 Tg) and SO_2 (0.5 Tg), (c) only H_2O ($\sim$ 150 Tg), and (d) only SO_2 (0.5 Tg). Simulations with the injection of SO_2 only (d) are optional and designed for aerosol-focused models. The SO_2 and water injections are prescribed based on Millán et al. (2022) and Carn et al. (2022). Note that $\sim$ 150 Tg of water is not the injection amount but the amount retained after the first couple of days. This is because some models form ice particles that fall out of the stratosphere due to large H_2O supersaturation during the initial injection (Zhu et al., 2022); these models will have to inject more H_2O to counterbalance the ice formation (see Table 6). The only requirement is that the model should have reasonable comparison to the MLS observations for water vapor, as shown in Fig. 1. Aside from retaining $\sim$ 150 Tg of water, the water vapor enhancement should be near 10 to 50 hPa, and most of the water vapor should be located between 10° N and 30° S by March 2022.

The first experiment (Exp1) is a free-running ensemble simulation covering the period from 2022 to 2031. The experiment has been designed to answer questions on the following:

1. understanding the long-term evolution of Hunga water vapor and aerosols in free-running models;
2. quantifying Hunga effects on stratospheric temperatures, dynamics, and transport;
3. understanding the impact of dynamic changes on ozone chemistry;
4. quantifying the net radiative effects;
5. estimating surface impacts (e.g., temperature, El Niño–Southern Oscillation, monsoon precipitation).

Simulations with free-running meteorology are required to properly understand the impacts of the eruption on atmospheric dynamics and transport processes and the resulting impacts of those on chemical species (e.g., ozone) and surface climate. Since coupling of the atmosphere with ocean

and land processes is required to fully simulate many aspects of the surface impacts, the use of coupled atmosphere, ocean, and land models is recommended. However, since such a fully interactive setup imposes additional computing requirements, an alternative model setup with fixed sea-surface temperatures (SSTs) and sea ice is also allowed. In that case, the prescribed climatological SSTs and sea-ice data are obtained by averaging SST during the past decade (2012–2021), with the same data imposed in both the $H_2O + SO_2$ (b) and control (a) simulations. It is important to note that both initial and boundary conditions in a model come with uncertainties, and model processes are simplified. Therefore, model simulations are influenced by the characteristics of the model itself and the background state of the atmospheric system (Jones et al., 2016; Brodowsky et al., 2021). To address some of the inherent uncertainties and reduce contribution of interannual variability to the forced response, we use a large ensemble of simulations with slightly varied initial conditions. Note that in the projection of stratospheric volcanic forcing, we only considered the Hunga eruption since 2022, and no future explosive eruptions are included. For example, the 2024 Mt. Ruang eruption contributed to elevated stratospheric aerosol optical depth, but it is not included.

Particularly, the first 5 years of qualified model output of Exp1 is used to understand climate impacts on the mesosphere and ionosphere from 2022–2027, such as gravity wave drag, temperature changes, polar mesospheric clouds (PMCs), and atmospheric circulation. The qualified models need to resolve the upper atmosphere with vertical resolutions higher than or equal to what we request in Sect. 3.

Since some aspects of the response, e.g., impacts on the radiative effect, may be too noisy from free-running model simulations even with large ensembles, we have also designed the second experiment, which uses nudged temperature and meteorology to ensure that the meteorology will be as close as possible to the one observed and thus isolate chemical changes and their radiative effect. Experiment 2 (Exp2) is a 2-year simulation that runs from 2022 to 2023 with nudged winds and/or temperature to answer questions on H_2O and aerosol evolution, quantification of the net radiative effects, and impacts on mid-latitude and polar ozone chemistry. Exp2 has two distinct realizations: Experiment 2a (Exp2a) and Experiment 2b (Exp2b). The models participating in Exp2a all have a prognostic aerosol module but vary in the complexity of their representation of aerosol microphysics (i.e., bulk, modal, or sectional). Models participating in Exp2b use prescribed aerosol surface area density (SAD) and radiative properties as input to the models (Jörimann et al., 2025). The prescribed aerosol properties are calculated using Global Space-based Stratospheric Aerosol Climatology (GloSSAC; Thomason et al., 2018; Kovilakam et al., 2020, 2023) version 2.22 aerosol data from 1979–2023. Note that for the period after the Hunga eruption, GloSSAC uses the Stratospheric Aerosol and Gas Experiment (SAGE-II/ISS) version 5.3 interpolated along the time axis and the Optical Spectrograph and InfraRed Imager System (OSIRIS) version 7.3 to fill in any missing data poleward of 60° N/S due to the unavailability of the Cloud-Aerosol Lidar and Infrared Pathfinder Satellite Observations (CALIPSO) data since January 2022. Therefore, when conducting analyses north/south of 60° N/S it should be noted that the aerosols may be underestimated due to the OSIRIS instrument retrieval biases. We ask for the models to check their initial chemical fields against the MLS to see if the models are qualified to evaluate their ozone chemistry. The nudged runs of Exp2 enable isolation of the chemical impact of the Hunga eruption from the volcanically induced changes in dynamics by comparing the runs with and without $H_2O + SO_2$ injection. The net radiative effect anomaly due to water and sulfate aerosol can also be calculated by comparing the control run (a) with the $H_2O + SO_2$ injection run (b).

Table 1 shows the forcings and emissions data used for the HTHH-MOC experiments. Table 2 shows the settings specific to each experiment. For volcanic injection for Exp1 and 2, we recommend the injections of H_2O and SO_2 at 04:00 UTC on 15 January 2022. All the models are required to retain a similar amount of water as observed by the MLS (~ 150 Tg). The models are recommended to compare with the MLS evolution for validation (Fig. 1). The goal is to retain the same amount of water and similar altitude to start with, so we can analyze the water's impact on the stratosphere and climate. If injecting 25–30 km cannot retain 150 Tg, models can inject higher than 30 km. The SO_2 injection is required to be 0.5 Tg for all models. The injection locations are not required to be co-injected with H_2O.

The data analysis of this project is designed to do inter-model comparisons, as well as inter-experiment comparisons. For example, the comparisons between Exp2a and Exp2b can help to understand how well we simulate the sulfate SAD and the importance of SAD variation for stratospheric ozone chemistry. Comparing Exp1 and Exp2 for the same period can help understand instantaneous and adjusted radiative effects. In addition, large (10–20) member ensembles are requested for free-running simulations to better quantify the role of internal variability in the climate response.

A parallel model intercomparison project Tonga-MIP (Clyne, 2024) will also be part of the 2025 Hunga assessment, which is designed to explore the plume evolution between 1 d and up to 1 or 2 months after the eruption. Tonga-MIP was initiated before the APARC Hunga Activity started. It will be described in a separate paper, but we list it in this paper to document the comprehensiveness of the modeling effort for the Hunga assessment. Two purposes of Tonga-MIP cannot be achieved by Exp1 and 2:

1. The nudged experiment of Tonga-MIP aims to intercompare the microphysics processes (i.e., cloud and aerosol physics and sulfur chemistry) between different models. Therefore, all models are requested to inject

Table 1. Summary of forcings and emissions data used in HTHH-MOC experiments.

Spin-up[a]	5-year nudged runs
Degassing[b] and eruptive volcano source	Need both degassing and eruptive volcanic input for 5-year spin-up. Degassing continues during the experiment runs (e.g., 10 years for Exp1, 2 years for Exp2). Recommended references: volcanic degassing (Carn et al., 2016, 2017); eruptive volcanoes (Neely and Schmidt, 2016; https://archive.researchdata.leeds.ac.uk/96/, last access: 12 August 2025; or Carn et al., 2017). Assume no more explosive volcanoes after Hunga.
Surface emission	Coupled Model Intercomparison Project phase 6 (CMIP6) emissions follow SSP2-4.5 (Gidden et al., 2019), which adopts an intermediate greenhouse gas (GHG) emission: CO_2 emissions around current levels before beginning to decline by 2050.
Chemical initialization	Stratospheric chemistry fields (such as O_3, H_2O) at the beginning of 2022 should be compared with MLS observations for validation if the model participates in evaluation of the Hunga stratospheric chemistry impact.

[a] 5 years is enough to reach sulfate equilibrium in the stratosphere; water may take 7 years (each model should adjust the spin-up time according to model features).
[b] Recommended degassing volcanic emissions injected at the cone altitude, constant flux based on Carn et al. (2017). Database is updated through 2022 here: https://doi.org/10.5067/MEASURES/SO2/DATA406 (Carn, 2022)

Table 2. Experiment design.

Experiment	Meteorology	Period	Aerosol treatment	QBO	SST	Ensemble members
Exp1.FixedSST	Free run starts 1 Feb (i.e., nudge until 31 Jan)	10 years 2022–2031 (first 5 years for mesospheric analysis)	Model-simulated aerosol or prescribed	Internally generated (nudge if model does not generate)	Fixed (climatology = mean of monthly average during the past decade (2012–2021), repeating annually). This applies to spin-up time too.	10–20
Exp1.CoupledOcean					Coupled ocean (optional), initialized with observed ocean state (see Sect. 3 for individual model descriptions)	10–20
Exp2a	Nudged wind only and/or nudged T and wind	2 years 2022–2023	Model-simulated aerosol	Nudged	Observed SST	1
Exp2b	Nudged wind only and/or nudged T and wind	2 years 2022–2023	Prescribed	Nudged	Observed SST	1

150 Tg of water, but the retaining of the water varies between models, differing from Exp1 and 2, which ask to retain ∼ 150 Tg of water in the stratosphere. SO_2 injection is 0.5 Tg, the same as experiments in HTHH-MOC. The injections are required to be injected between 25–30 km, within the latitude and longitude box of 22–14° S and 182–186° E, at a constant vertical volume mixing ratio for 6 h starting at 04:00 UTC on 15 January.

2. The free-run experiment of Tonga-MIP aims to study the radiative effect of water and SO_2 on the Hunga plume descending and ascending during the first month after the eruption since the Hunga water and aerosol plumes were observed to descend several kilometers during the first monthly after the eruption (Sellito et al., 2022; Randel et al., 2024). Therefore, Tonga-MIP designed to nudge the atmosphere up until several different dates and explore the plume descending patterns with free-run atmosphere after these dates. The dates are

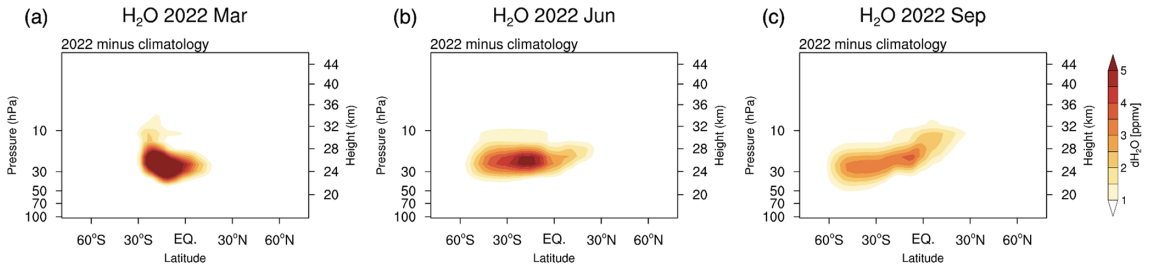

Figure 1. Monthly average water vapor perturbation after the Hunga eruption from MLS. Panels **(a)**–**(c)** show the observed dispersion of the H_2O enhancement in 2022 in the months of **(a)** March, **(b)** June, and **(c)** September.

21, 26, and 31 January. Most of the models that participate in Tonga-MIP also participate in the HTHH-MOC.

3 Model output

The model output covers variables based on the Chemistry-Climate Modeling Initiative (CCMI) output list, with some additions specific to this study. The detailed list is provided in Tables S1–S5 in the Supplement. We have requested that all models generate the same variable names, units, ordering of dimensions (longitude from 0 to 360° E, latitude from 90° S to 90° N, pressure levels from 1000 to 0.03 hPa, or altitude from 0 to 73 000 m), and file name structure (e.g., "variable_domain_modelname_experimentname.nc" or "domain_modelname_experimentname.variable.nc"). Examples of Experiment_name are HTHHMOC-Exp1 and HTHHMOC-Exp1. Example file names are Monthlymean_WACCM6MAM_HTHHMOC-Exp1-NoVolc-fixedSST.ensemble001.O3.nc or O3_Dailymean_WACCM6MAM_HTHHMOC-Exp1-H2Oonly-CoupledOcean.ensemble001.nc.

The 3D model output is requested on both model levels (hybrid pressure or height) and interpolated to CMIP6 plev39 grid (plev39: 1000, 925, 850, 700, 600, 500, 400, 300, 250, 200, 170, 150, 130, 115, 100, 90, 80, 70, 50, 30, 20, 15, 10, 7, 5, 3, 2, 1.5, 1 0, 0.7, 0.5, 0.4, 0.3, 0.2, 0.15, 0.1, 0.07, 0.05, 0.03 hPa) and for mesospheric analysis adding 0.02, 0.01, 0.007, 0.005, 0.003, and 0.001 above the plev39 grid.

Monthly mean output is requested for all variables for Exp1 with some fields (specified in the Excel sheet) as daily mean. Some of the fields requested as daily means are specified, either as surface fields or at a reduced number of pressure levels. Daily mean output is requested for all variables for Exp2.

The model output (∼ 33 TB) of Exp1 and Exp2 is archived at the JASMIN workspace (https://jasmin.ac.uk, last access: 12 August 2025). JASMIN provides large storage space and compute facilities to facilitate the data archiving and post-data analysis of this project. This reduces the need for data transfers and allows reproducible computational workflows. Seddon et al. (2023) described the facility in detail. Our next phase is to publicly release the data by transferring the data to the Centre for Environmental Data Analysis (CEDA) archiving system.

4 Model descriptions and the Hunga volcanic injection specification

As part of the 3-year Hunga Impact activity, this project is highly time-sensitive. We designed the timeline for each experiment (Fig. 2) to facilitate the completion of the 2025 Hunga Impact assessment. However, the JASMIN workspace will remain open for the uploading of modeling data after the deadline denoted in Fig. 2 until 2025.

This paper only includes model descriptions for those models that submitted the output following the assessment timeline. The model setup follows the protocols listed in Sect. 2 unless specified below. Tables 3–6 provide key information on the participant models, which are described in detail in the following paragraphs for each model.

4.1 CAM5/CARMA

The atmospheric component of the Community Atmosphere Model version 5 (CAM5) (Lamarque et al., 2012) is the atmospheric component of the Community Earth System Model, version 1 (CESM1.2.2, Hurrell et al., 2013), with a top at around 45 km. CAM5 has a horizontal resolution of 1.9° latitude × 2.5° longitude, utilizing the finite-volume dynamical core (Lin and Rood, 1996). The model has 56 vertical levels, with a vertical resolution ∼ 1 km in the upper troposphere and lower stratosphere. The modeled winds and temperatures were nudged to the 3 h Goddard Earth Observing System 5 (GEOS-5) reanalysis dataset (Molod et al., 2015) every time step (30 min) by 1 % (i.e., a 50 h Newtonian relaxation timescale). The aerosol is interactively simulated using a sectional aerosol microphysics model, the Community Aerosol and Radiation Model for Atmospheres (CARMA, Yu et al., 2015). The model uses the Model for Ozone and Related Chemical Tracers (MOZART) chemistry that is used for both tropospheric (Emmons et al., 2010) and stratospheric chemistry (English et al., 2011; Mills et al., 2016). The volcanic emissions from continuously degassing

Table 3. Participating models and contact information for HTHH-MOC and Tonga-MIP.

Model name	Description reference paper	Institutions (that develop the model)	Primary contact (who runs the model)	Emails
CAM5/CARMA	Yu et al. (2015)	CU Boulder, Jinan Univ.	Pengfei Yu, Yifeng Peng	pengfei.yu@colorado.edu, pengyf16@lzu.edu.cn
CCSRNIES-MIROC3.2	Akiyoshi et al. (2023, 2016)	NIES	Yousuke Yamashita, Hideharu Akiyoshi	yamashita.yosuke@nies.go.jp, hakiyosi@nies.go.jp
CMAM	Jonsson et al. (2004), Scinocca et al. (2008)	CCCma, Environment and Climate Change Canada	David Plummer	david.plummer@ec.gc.ca
EMAC MPIC	Schallock et al. (2023)	MPI-C, -M, DLR	Christoph Brühl	christoph.bruehl@mpic.de
GA4 UM-UKCA	Dhomse et al. (2020)	Univ. Leeds	Graham Mann, Sandip Dhomse	g.w.mann@leeds.ac.uk, s.s.dhomse@leeds.ac.uk
GEOSCCM	Nielsen et al. (2017)	NASA	Peter Colarco	peter.r.colarco@nasa.gov
GEOS/CARMA	Nielsen et al. (2017)	NASA	Parker Case	parker.a.case@nasa.gov
GSFC2D	Fleming et al. (2024)	NASA	Eric Fleming	eric.l.fleming@nasa.gov
IFS-COMPO Cy49R1	Huijnen et al. (2016), Rémy et al. (2022)	ECMWF and team CAMS2_35	Simon Chabrillat, Samuel Rémy	simon.chabrillat@aeronomie.be sr@hygeos.com
LMDZ6.2-LR-STRATAER/LMDZ6.2-LR-STRATAER-REPROBUS	Boucher et al. (2020), Marchand et al. (2012)	CNRS, Sorbonne Univerité, IPSL, LATMOS, LOCEAN	Marion Marchand, Slimane Bekki, Nicolas Lebas, Lola Falletti	marion.marchand@latmos.ipsl.fr, slimane.bekki@latmos.ipsl.fr, nicolas.lebas@locean.ipsl.fr, lola.falletti@latmos.ipsl.fr
MIROC-CHASER	Sekiya et al. (2016)	JAMSTEC	Shingo Watanabe, Takashi Sekiya	wnabe@jamstec.go.jp, tsekiya@jamstec.go.jp
MIROC-ES2H	Tatebe et al. (2019), Kawamiya et al. (2020)	JAMSTEC and NIES	Shingo Watanabe, Takashi Sekiya, Tatsuya Nagashima, Kengo Sudo	wnabe@jamstec.go.jp, tsekiya@jamstec.go.jp, nagashima.tatsuya@nies.go.jp, kengo@nagoya-u.jp
SOCOLv4	Sukhodolov et al. (2021)	PMOD/WRC and ETH-Zurich	Timofei Sukhodolov	timofei.sukhodolov@pmodwrc.ch
UKESM1.1	Sellar et al. (2019, 2020), with chemistry updates from Dennison et al. (2019)	UK Met Office, UK Universities, and National Centre for Atmospheric Science (NCAS)	Graham Mann, Sandip Dhomse, Ben Johnson, Mohit Dalvi, Luke Abraham, James Keeble	g.w.mann@leeds.ac.uk, s.s.dhomse@leeds.ac.uk, ben.johnson@metoffice.gov.uk, mohit.dalvi@metoffice.gov.uk, nla27@cam.ac.uk, j.keeble2@lancaster.ac.uk
WACCM6/CARMA	Tilmes et al. (2023)	NCAR	Simone Tilmes, Cheng-Cheng Liu, Yunqian Zhu, Margot Clyne (Tonga-MIP)	tilmes@ucar.edu, cheng-cheng.liu@outlook.com, yunqian.zhu@noaa.gov, margot.clyne@colorado.edu

Table 3. Continued.

Model name	Description reference paper	Institutions (that develop the model)	Primary contact (who runs the model)	Emails
WACCM6/MAM	Mills et al. (2016)	NCAR	Xinyue Wang, Simone Tilmes, Jun Zhang, Wandi Yu, Zhihong Zhuo, Ewa Bednarz, Margot Clyne (Tonga-MIP)	xinyuew@colorado.edu, tilmes@ucar.edu, jzhan166@ucar.edu, yu44@llnl.gov, zhuo.zhihong@uqam.ca, ewa.bednarz@noaa.gov, margot.clyne@colorado.edu

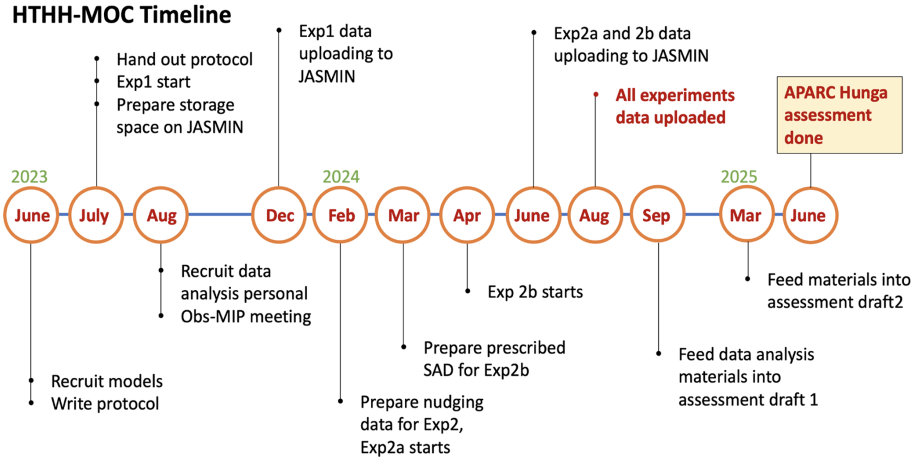

Figure 2. The timeline designed for HTHH-MOC in order to cooperate with the APARC HTHH Impact assessment.

volcanoes use the emission inventory RCP8.5 and FINNv1.5. No volcanic eruptions except the Hunga 2022 eruption are included.

The initial volcanic injection altitude and area are determined by validating the water and aerosol transportation in months shown in Fig. 1 following the tests in Zhu et al. (2022), Wang et al. (2023), and Zhang et al. (2024). In these simulations, the H_2O is injected at 25 to 35 km altitude, and SO_2 is injected at 20 to 28 km altitude. The injection latitude ranges from 22 to 14° S, and longitude ranges from 182 to 186° E (Zhu et al., 2022). The initial injection of H_2O is 150 Tg, with ∼ 135 Tg left after the first week following the eruption.

4.2 CCSRNIES-MIROC3.2

The Center for Climate System Research/National Institute for Environmental Studies-Model for Interdisciplinary Research on Climate version 3.2 Chemistry Climate Model (CCSRNIES-MIROC3.2 CCM) (Akiyoshi et al., 2023) was developed based on version 3.2 of the MIROC atmospheric general circulation model (AGCM), incorporating a stratospheric chemistry module that was developed at the National Institute for Environmental Studies (NIES) and the University of Tokyo. The model has a horizontal resolution of T42 (2.8° latitude × 2.8° longitude) and 34 vertical levels, with a vertical resolution ∼ 1 km in the lower stratosphere–upper troposphere and ∼ 3 km in the upper stratosphere and mesosphere. The top level is located at 0.01 hPa (approximately 80 km).

The chemistry in the CCSRNIES-MIROC3.2 CCM is a stratospheric chemistry module including 42 photolysis reactions, 142 gas-phase chemical reactions, and 13 heterogeneous reactions for multiple aerosol types (Akiyoshi et al., 2023). Tropospheric chemistry is not included, but the stratospheric chemistry scheme is used for both the troposphere and the mesosphere.

In the CCSRNIES-MIROC3.2 CCM, only Exp2b can be performed. The atmospheric temperature and horizontal winds are nudged toward Modern-Era Retrospective analysis for Research and Applications Version 2 (MERRA-2) reanalysis (Gelaro et al., 2017) with a 1 d relaxation using instant values at 6 h interval (Akiyoshi et al., 2016). The HadISST data are used during the simulation.

The CCSRNIES-MIROC3.2 CCM does not have any microphysics scheme for volcanic aerosols. The surface area and spectral optical parameters of extinction, single scattering albedo, and asymmetric factor for Hunga aerosols were

Table 4. Participating models in HTHH-MOC and Tonga-MIP.

Model names	Exp1.FixedSST	Exp1.CoupledOcean	Exp2a	Exp2b	Tonga-MIP (Clyne, 2024)
CAM5/CARMA			×		
CCSRNIES-MIROC3.2				×	
CMAM	× (H_2O-only)(*)				
EMAC MPIC			×		
GA4 UM-UKCA					×
GEOSCCM	×		×		×
GEOS/CARMA			×		
GSFC2D	×(*)			×	
IFS-COMPO			×		
LMDZ6.2-LR-STRATAER			×		×
LMDZ6.2-LR-STRATAER-REPROBUS			×		×
MIROC-CHASER	×		×		
MIROC-ES2H					×
SOCOLv4					×
UKESM1.1			×		×
WACCM6/CARMA			×		×
WACCM6/MAM	×(*)	×(*)	×		×

* The models that are qualified to analyze the mesospheric components are marked with the * symbol.

prescribed in the model from the GloSSAC version 2.22 aerosol data (Jörimann et al., 2025). H_2O was injected instantly on 15 January 2022 at the 12 grids of the model in the region 181.4–187.0° E in longitude, 14.0–22.3° S in latitude, and 12.0–27.6 hPa in pressure level. A uniform number density of 1.709×10^{15} molec. cm^{-3} H_2O was injected in each of the 12 grids, which amounts to $\sim$ 150 Tg.

4.3 CMAM

The Canadian Middle Atmosphere Model (CMAM) is based on a vertically extended version of CanAM3.1, the third-generation Canadian Atmospheric Model (Scinocca et al., 2008). Compared to the standard configuration of CanAM3.1, for CMAM the model top was raised to 0.0006 hPa (approximately 95 km), and the parameterization of non-orographic gravity wave drag (Scinocca, 2003) and additional radiative processes important in the middle atmosphere (Fomichev et al., 2004) have been included. The gas-phase chemistry includes a comprehensive description of the inorganic O_x, NO_x, HO_x, ClO_x, and BrO_x families, along with CH_4, N_2O, six chlorine-containing halocarbons, CH_3Br and, to account for an additional 5 ppt of bromine from short-lived source gases, CH_2Br_2 and $CHBr_3$ (Jonsson et al., 2004). A prognostic description of, and associated heterogeneous chemical reactions on, water ice PSCs (PSC Type II) and liquid ternary solution (PSC Type Ib) particles is included, although gravitational settling (dehydration/denitrification) is not calculated, and species return to the gas phase when conditions no longer support the existence of PSC particles.

The simulations for the HTHH-MOC simulations were performed at T47 spectral resolution (approximately 3.8° resolution on the linear transform grid used for the model physics), with 80 vertical levels giving a vertical resolution of approximately 0.8 km at 100 hPa, increasing to 2.3 km above 0.1 hPa. The CMAM does not internally generate a QBO, so the zonal winds in the equatorial region were nudged towards a dataset based on observed variations up to December 2023, constructed using the method of Naujokat (1986) and extended into the future by repeating a historical period that is congruent with the observed QBO in late 2023. Water vapor from the Hunga eruption was added as a zonally averaged perturbation to the model water over 5 d from 00:00 UTC on 20 February 2022. The spatial distribution of the anomaly was designed to reproduce the water vapor anomaly observed

Table 5. Model resolutions and schemes used for HTHH-MOC experiments.

Model names	Horizontal resolution	No. of levels	Model top	Vertical resolution in the stratosphere	Aerosol scheme	Specified dynamic source	QBO for models participating free run	Chemistry package (tropospheric chemistry included?)
CAM5/CARMA	∼ 2°	56	45 km	1–4 km	CARMA sectional (20 bins)	GEOS5	–	MOZART (yes)
CCSRNIES-MIROC3.2	T42	34	0.01 hPa	1–3 km	None	MERRA-2	–	full strat; no tropo
CMAM	T47	80	0.0006 hPa	0.8–2.5 km	None	ERA5	Nudged	stratospheric + methane–NO_x in troposphere
EMAC MPIC	T63	90	0.01 hPa	0.5 km in LS	GMXE, modal	ERA-5	–	MECCA, simplified troposphere
GEOSCCM	c90 (∼ 1°)	72	0.01 hPa	∼ 1 km	GOCART (bulk)	MERRA-2/GEOS-FP	Internally generated	GMI (yes)
GEOS/CARMA	c90 (∼ 1°)	72	0.01 hPa	∼ 1 km	CARMA (sectional 24 bins)	MERRA-2/GEOS-FP	–	GMI (yes)
GSFC2D	4°	76	0.002 hPa (∼ 92 km)	1 km	Prescribed only	MERRA-2	Internally generated	full strat; partial trop
IFS-COMPO	T_L511 (∼ 40 km)	137	0.01 hPa	0.5–1.5 km	Bulk	ERA5	–	BASCOE (strato) + CB05 (tropo)
LMDZ6.2-LR-STRATAER	2.5° × 1.3°	79	80 km	1–5 km	S3A (sectional 36 bins)	ERA5	–	No
LMDZ6.2-LR-STRATAER-REPROBUS	2.5° × 1.3°	79	80 km	1–5 km	S3A(sectional 36 bins)	ERA5	–	REPROBUS
MIROC-CHASER	T85	81	0.004 hPa	0.7–1.2 km	MAM3	MERRA-2	Internally generated	troposphere–stratosphere chemistry
UKESM1.1	N96	85	80 km	0.6–0.7 km in LS	GLOMAP-mode	ERA-5	Internally generated	CheST strat-trop chemistry
WACCM6/CARMA	∼ 1°	70	140 km	1–2 km	Sectional (20 bins)	MERRA-2	–	MOZART (yes)
WACCM6/MAM	∼ 1°	70	140 km	1–2 km	MAM4	MERRA-2	Internally generated	MOZART (yes)

in mid-February by the Atmospheric Chemistry Experiment – Fourier Transform Spectrometer (ACE-FTS) (Bernath et al., 2005) satellite (Patrick Sheese, personal communication, 2022), with a maximum value of 13.3 ppm at 17° S and 25.5 km and producing an anomaly of ∼ 150 Tg H_2O in the stratosphere.

4.4 EMAC MPIC

The chemistry–climate model EMAC (ECHAM5/MESSy Atmospheric Chemistry) consists of the European Centre Hamburg general circulation model (ECHAM5) and the Modular Earth Submodel System (MESSy) (e.g., Jöckel et al., 2010). Here we use the version of Schallock et al. (2023) in horizontal resolution T63 (1.87° × 1.87°) with 90 levels between the surface and 0.01 hPa.

Table 6. Hunga volcanic injection profile for HTHH-MOC experiments.

Model names	Data and duration	H_2O amount (left after a week)	H_2O altitude	H_2O location/area	SO_2 amount	SO_2 altitude	SO_2 location/area
CAM5/CARMA	15 Jan, 6 h	150 Tg (∼ 135 Tg)	25–35 km	22–14° S, 182–186° E	0.5 Tg	20–28 km	22–14° S, 182–186° E
CCSRNIES-MIROC3.2	15 Jan, instantly	150 Tg (∼ 150 Tg)	12.0–27.6 hPa	181.4–187.0° E, 14.0–22.3° S	–	–	–
CMAM	20 Feb, 5 d	150 Tg (∼ 150 Tg)	near 25.5 km	zonally averaged	–	–	–
EMAC MPIC	16 Jan, 12 h	136 Tg (∼ 130 Tg)	Gaussian-centered at 21.5 hPa	23–19° S, 177–173° W	0.4 Tg based on obs.	23–27 km based on obs.	30° S–5° N, 90–120° W (330°)
GEOSCCM	15 Jan, 6 h	750 Tg (∼ 150 Tg)	25–30 km	22–14° S, 182–186° E	0.5 Tg	25–30 km	22–14° S, 182–186° E
GEOS/CARMA	15 Jan, 6 h	750 Tg (∼ 150 Tg)	25–30 km	22–14° S, 182–186° E	0.5 Tg	25–30 km	22–14° S, 182–186° E
GSFC2D	use MLS H_2O profile until 1 March	∼ 150 Tg (∼ 150 Tg)	–	zonally averaged	–	–	–
IFS-COMPO	15 Jan, 3 h	190 Tg (∼ 150 Tg)	25–30 km	400 km by 200 km centered 20° S and 175° W	0.5 Tg	25–30 km	400 km by 200 km centered 20° S and 175° W
LMDZ6.2-LR-STRATAER	15 Jan, 1 d	150 Tg (∼ 150 Tg)	Gaussian-centered at 27.5 km and standard deviation of 2.5 km	22–14° S, 182–186° E	0.5 Tg	Gaussian-centered at 27.5 km and standard deviation of 2.5 km	22–14° S, 182–186° E
LMDZ6.2-LR-STRATAER-REPROBUS	15 Jan, 1 d	150 Tg (∼ 150 Tg)	Gaussian-centered at 27.5 km and standard deviation of 2.5 km	22–14° S, 182–186° E	0.5 Tg	Gaussian-centered at 27.5 km and standard deviation of 2.5 km	22–14° S, 182–186° E
MIROC-CHASER	15 Jan, 04:00 UTC, 6 h	186 Tg (∼ 150 Tg)	25–30 km	22–14° S, 182–186° E	0.5 Tg	25–30 km	22–14° S, 182–186° E
UKESM1.1	15 Jan, 6 h	150 Tg	25–30 km	22–14° S 182–186° E	0.5 Tg	25–30 km	22–14° S, 182–186° E
WACCM6/CARMA	15 Jan, 6 h	150 Tg (∼ 150 Tg)	25–35 km	22–6° S, 182.5–202.5° E	0.5 Tg	26.5–36 km	22–6° S, 182.5–202.5° E
WACCM6/MAM	15 Jan, 6 h	150 Tg (∼ 135 Tg)	25-35 km	22–14° S, 182–186° E	0.5 Tg	20–28 km	22–14° S, 182–186° E

Vorticity, divergence, and temperatures between surface and 100 hPa are nudged to the ERA5 reanalysis of ECMWF (Hersbach et al., 2020), as well as surface pressure. SSTs and sea ice cover are prescribed by ERA5 data. The model can generate an internal QBO, but for comparison with observations it was slightly nudged to the Singapore data compiled by the Free University of Berlin and Karlsruhe Institute of Technology (Giorgetta et al., 2006).

The model contains gas-phase and heterogeneous chemistry on PSCs and interactive aerosols. Surface mixing ratios of chlorine- and bromine-containing halocarbons and other long-lived gases are nudged to Advanced Global Atmospheric Gases Experiment (AGAGE) observations. The microphysical modal aerosol module contains four soluble and three insoluble modes for sulfate, nitrate, dust, organic and black carbon, and aerosol water (Pringle et al., 2010). The instantaneous radiative effect by tropospheric and stratospheric aerosols can be calculated online by multiple calls of the radiation module. Volcanoes injecting material into the stratosphere are considered as in Schallock et al. (2023) using the perturbations of stratospheric SO_2 observed by the Michelson Interferometer for Passive Atmospheric Sounding (MIPAS) and aerosol extinction observed by OSIRIS. This method, based typically on data of a 10 d period, distributes the injected SO_2 over a larger volume than typical point source approaches using the same integrated mass (see also Kohl et al., 2025). For Hunga this method has the disadvantage that H_2O and SO_2 are not co-injected since H_2O is injected in 12 h in a slab consisting of four horizontal boxes and a Gaussian vertical distribution centered at 21.5 hPa. For Exp2a we continue the 30-year transient simulation presented in Schallock et al. (2023) with and without Hunga Tonga. The simulated H_2O perturbation is consistent with Fig. 1. The SO_2 injection is derived based on the extinction from the OSIRIS observation averaged over about 10 d (Fig. 3) (Bruehl et al., 2023).

4.5 GEOSCCM

The NASA Goddard Earth Observing System Chemistry-Climate Model (GEOSCCM) is based on the GEOS Earth system model (Reinecker et al., 2008; Molod et al., 2015). For the HTHH-MOC experiments the model is run on a cubed-sphere horizontal grid at a C90 resolution ($\sim$ 100 km) with 72 vertical hybrid-sigma levels from the surface to 0.01 hPa ($\sim$ 80 km). Dynamics are solved using the finite-volume dynamical core (Putman and Lin, 2007). Deep convection and shallow convection are parameterized using the Grell and Freitas (2014) and Bretherton and Park (2009) schemes, respectively, and moist physics is from Bacmeister et al. (2006). The turbulence parameterization is based on the non-local scheme of Lock et al. (2000). Shortwave and longwave radiative fluxes are computed in 30 bands using the Rapid Radiative Transfer Model for GCMs (RRTMG, Iacono et al., 2008).

Stratospheric chemistry and tropospheric chemistry are from the Global Modeling Initiative (GMI) mechanism (Duncan et al., 2007; Strahan et al., 2007; Nielsen et al., 2017), updated here to include reactions for sulfur species. The GMI mechanism in GEOSCCM has been extensively evaluated for its stratospheric ozone-related photochemistry and transport in various model intercomparisons, including Stratosphere-troposphere Processes and their Role in Climate (SPARC) Chemistry Climate Model Validation (CCMVal), CCMVal-2, and the CCMI (SPARC, 2010; Eyring et al., 2010, 2013; Morgenstern et al., 2017). Aerosol species are simulated by the Goddard Chemistry, Aerosol, Radiation, and Transport, second-generation (GOCART-2G) module (Collow et al., 2024), which includes a sectional approach for dust (five bins), sea salt (five bins), and nitrate (three bins) and a bulk approach for sulfate (dimethyl sulfide, SO_2, methanesulfonic acid, and SO_4^{2-}) aerosol and carbonaceous species (hydrophobic and hydrophilic modes of "white" and "brown" organics and black carbon).

For the GEOSCCM simulations performed with the GOCART-2G module we use the nominal GOCART-2G sulfate mechanism, updated here to use the online hydroxyl (OH) radical, nitrate (NO_3) radical, and hydrogen peroxide (H_2O_2) from the GMI mechanism instead of climatological fields provided from offline files (Collow et al., 2024). While not a full coupling to the GMI sulfur cycle it nevertheless allows the GOCART-2G sulfate mechanism to have the impact of the Hunga water vapor perturbation on the oxidants. A second "instance" of the GOCART-2G sulfate mechanism is run that is specifically for the volcanic SO_2 and resultant sulfate from the Hunga eruption. This allows us to track the eruptive volcanic aerosol separately from the nominal sulfate instance that sees mainly tropospheric sources. We assign this volcanic instance optical properties consistent with SAGE retrievals of the sulfate aerosol properties, using an effective radius of 0.4 µm. We find that 750 Tg of H_2O is needed in the initial injection to provide a residual $\sim$ 150 Tg of water in the stratosphere after a week. All other injection parameters follow the protocol. The model spin-up was performed by "replaying" to the MERRA-2 meteorology (Gelaro et al., 2017), and is used throughout the Exp2a results. A MERRA-2 2012–2021 climatology of SST and sea ice fractions are used based on Reynolds et al. (2002).

4.6 GEOS/CARMA

A second configuration of the GEOSCCM, coupled to the sectional aerosol microphysics package CARMA, also simulated the eruption (GEOS/CARMA). This configuration is the same as above except for the aerosol package and its coupling to the GMI chemistry mechanism. For this version of GEOSCCM, we use the configuration of CARMA described in Case et al. (2023). This configuration uses 24 size bins, spread logarithmically in volume between 0.25 nm and 6.7 µm in radius, and simulates the nucleation, conden-

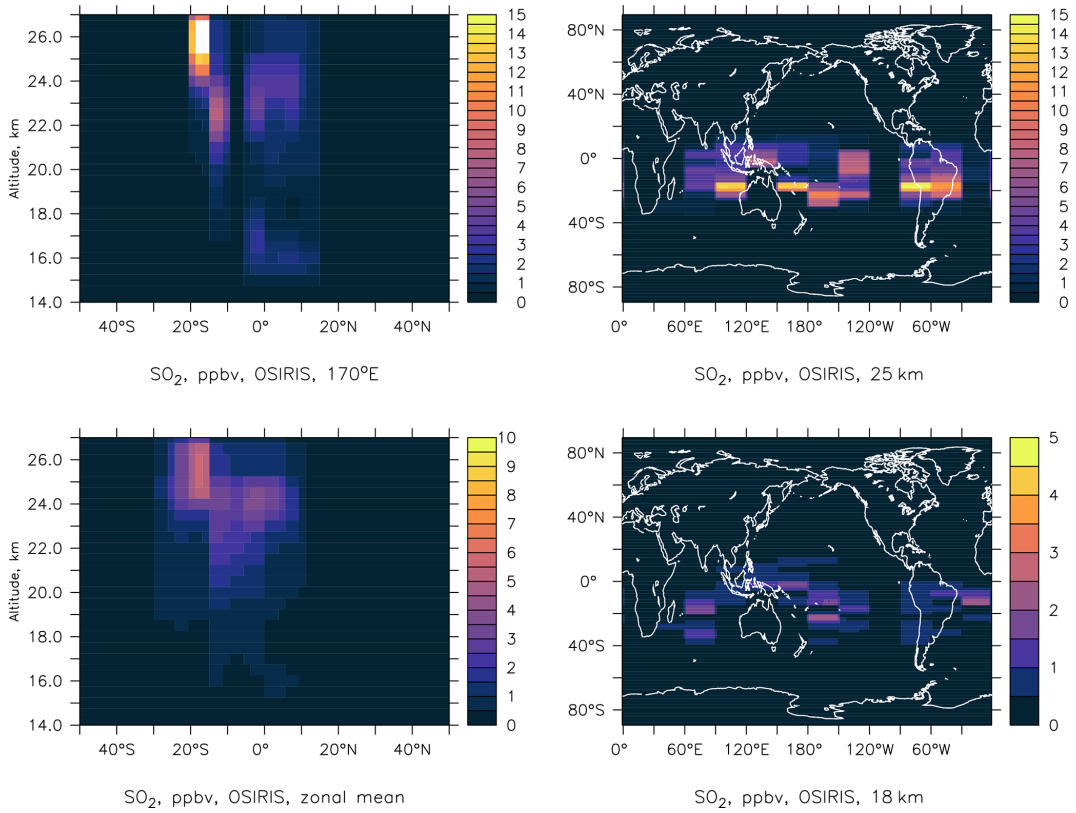

Figure 3. The SO_2 injection used in EMAC MPIC model is based on the Hunga SO_2 perturbation derived from extinction observed by OSIRIS averaged over about 10 d, i.e., including several snapshots of the westward-moving plume. For conversion from extinction to volume mixing ratio, Eq. (1) of Schallock et al. (2023) is applied with $f = 3$ because of data gaps. 5 d averaged gridded OSIRIS data averaged from 24 January at 00:00 UTC to 3 February at 00:00 UTC were used. Note that the color bars are not the same in each panel.

sational growth, evaporation, coagulation, and settling of sulfate aerosols in these simulations following the mechanism of English et al. (2013). For these simulations, CARMA is fully coupled to the GMI sulfur cycle by the production (i.e., oxidation of SO_2, evaporation of sulfate aerosols) and loss (i.e., nucleation and condensation of sulfate aerosols) of sulfuric acid (H_2SO_4) vapor. Optical properties for the CARMA aerosols are calculated based on the interactively calculated aerosol size distribution. The same injection parameters for GEOSCCM described above are used by this configuration. This model configuration contributed to Exp2a and "replayed" to MERRA-2 meteorology as above.

4.7 GSFC2D

The NASA/Goddard Space Flight Center two-dimensional (2D) chemistry–climate model (GSFC2D) has a domain extending from the surface to ∼ 92 km (0.002 hPa). The model has 76 levels, with 1 km vertical resolution from the surface to the lower mesosphere (60 km) and 2 km resolution above (60–92 km). The horizontal resolution is 4° latitude, and the model uses a 2D (latitude–altitude) finite-volume dynamical core (Lin and Rood, 1996) for advective transport. The model has detailed stratospheric chemistry and reduced tropospheric chemistry, with a diurnal cycle computed for all constituents each day (Fleming et al., 2024). The model uses prescribed zonal mean surface temperature as a function of latitude and season based on a multi-year average of MERRA-2 data (Gelaro et al., 2017). Zonal mean latent heating, tropospheric water vapor, and cloud radiative properties as a function of latitude, altitude, and season are also prescribed (Fleming et al., 2020).

For the free-running simulations, the model planetary wave parameterization (Bacmeister et al., 1995; Fleming et al., 2024) uses lower boundary conditions (750 hPa, ∼ 2 km) of geopotential height amplitude and phase for zonal wave numbers 1–4. These are derived as a function of latitude and season using (1) a 30-year average (1991–2020) of MERRA-2 data for the standard yearly repeating climatological-dynamics simulations ("Clim-NoQBO") and (2) individual years of MERRA-2 data (1980–2020), randomly rearranged in time to generate interannual variations in stratospheric dynamics ("ensemble1", "ensemble2", … "ensemble10"). For the inter-annually varying dynamics simulations, the model includes an internally generated QBO (Fleming et al., 2024).

For experiments that include the Hunga volcanic aerosols, the simulations go through the end of 2023, using prescribed aerosol properties for 2022–2023 both from the GloSSAC dataset and from the OMPS-LP data (Taha et al., 2021, 2022). For experiments that include the Hunga H_2O injection, Aura/MLS observations are used to derive a daily zonal mean Hunga water vapor anomaly in latitude–altitude, which is added to the baseline H_2O (no volcano) through the end of February 2022. This combined water vapor field is then fully model computed starting 1 March 2022 through the end of 2031.

For Exp2b, the model zonal mean temperature and transport fields are computed from the MERRA-2 reanalysis data. These are input into the model and used as prescribed fields (no nudging is done).

4.8 IFS-COMPO

The Copernicus Atmosphere Monitoring Service (CAMS) provides daily global analysis and 5 d forecasts of atmospheric composition (aerosols, trace gases, and greenhouse gases (GHGs)) (Peuch et al., 2022). CAMS is coordinated by the European Centre for Medium Range Weather Forecasts (ECMWF) and uses, for its global component, the Integrated Forecasting System (IFS), with extensions to represent aerosols, trace, and GHGs, being called "IFS-COMPO" (also previously known as "C-IFS", Flemming et al., 2015). IFS-COMPO is composed of IFS(AER) for aerosols, as described in Remy et al. (2022), while the atmospheric chemistry is based on the chemistry module as described in Williams et al. (2022) for the troposphere (IFS-CB05) and Huijnen et al. (2016) for the stratosphere (IFS-CBA). The stratospheric chemistry module of IFS-COMPO is derived from the Belgian Assimilation System for Chemical ObsErvations (BASCOE, Errera et al., 2019). IFS-COMPO stratospheric chemistry is used since the operational implementation of cycle 48R1 on 27 June 2023 (Eskes et al., 2024).

The aerosol component of IFS-COMPO is a bulk aerosol scheme for all species except sea salt aerosol and desert dust, for which a sectional approach is preferred, with three bins for each of these two species. Since the implementation of operational cycle 48R1 in June 2023, the prognostic species are sea salt, desert dust, organic matter (OM), black carbon (BC), sulfate, nitrate, ammonium, and secondary organic aerosols (SOAs).

For Exp2a, cycle 49R1 IFS-COMPO has been used, which will become operational for CAMS production in November 2024, at a resolution of TL511 (∼ 40 km grid cell) over 137 model levels from surface to 0.01 hPa. Cycle 49R1 IFS-COMPO integrates a number of updates of tropospheric and stratospheric aerosols and chemistry. The most relevant aspect for this work concerns the representation of stratospheric aerosols, which has been revisited with the implementation of a coupling to the stratospheric chemistry through a simplified stratospheric sulfur cycle including nucleation/condensation and evaporation processes, as shown in Fig. 4. Direct injection of water vapor into the stratosphere is expected to enhance the nucleation and condensation of sulfate through the reaction with SO_3 and production of gas-phase H_2SO_4.

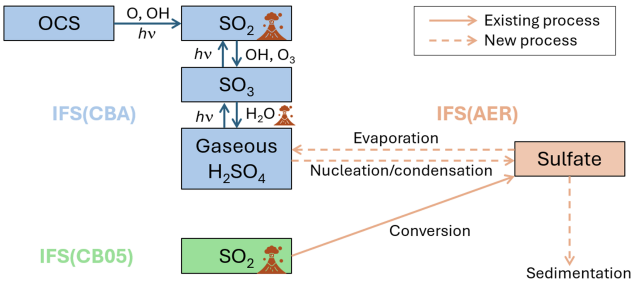

Figure 4. Architecture of the stratospheric extension of IFS(AER) and its coupling with IFS(CBA) and IFS(CB05), with existing and new processes implemented in cycle 49R1 of IFS-COMPO. $h\nu$ represents photolysis, and the volcano symbols represent direct injections by volcanic eruptions. Sedimentation is indicated as a new process because it has been revisited.

The volcanic injection takes place between 03:00 and 06:00 UTC on 15 January 2022, with a uniform vertical distribution between 25 and 30 km of altitude, over a rectangular region of 400 km (latitude) × 200 km (longitude) centered on the coordinates of the Hunga volcano. The injected quantities are 0.5 Tg SO_2 and 190 Tg H_2O.

4.9 LMDZ6.2-LR-STRATAER and LMDZ6.2-LR-STRATAER-REPROBUS

The Institut Pierre-Simon Laplace Climate Modelling Centre (IPSL CMC; see https://cmc.ipsl.fr, last access: 12 August 2025) has set up a new version of its climate model in the runup to CMIP6. Further description of the IPSL-CM6A-LR climate model can be found in Boucher et al. (2020) and in Lurton et al. (2020). New development of the model is now ongoing to prepare the IPSLCM7 version.

The IPSLCM7 climate model is using the general circulation model named LMDZ (Laboratoire de Météorologie Dynamique-Zoom; Hourdin et al., 2006). The LMDZ version used for this study is based on a regular horizontal grid with 144 points regularly spaced in longitude and 142 in latitude, corresponding to a resolution of 2.5° × 1.3°. The model has 79 vertical layers and extends up to 80 km, which makes it a "high-top" model. The model shows a self-generated quasi-biennial oscillation (QBO), whose period has been tuned to the observed one for the present-day climate (Boucher et al., 2020).

The aerosol is interactively simulated in the STRATAER module using a sectional scheme with 36 size bins. STRATAER is an improved version of the Sectional Stratospheric Sulfate Aerosol (S3A) module (Kleinschmitt et al., 2017). It now takes into account the photolytic conversion of

H_2SO_4 into SO_2 in the upper stratosphere (Mills et al., 2005). The size-dependent composition of H_2SO_4/H_2O aerosols is now computed iteratively to ensure that the surface tension, density, and composition are consistent in the calculation of the Kelvin effect. The surface tension, density, H_2SO_4 vapor pressure, and nucleation rates are calculated based on Vehkamäki et al. (2002). The version of the LMDZ6.2-LR-STRATAER atmospheric model used in the HTHH Impact project accounts for the stratospheric H_2O source from methane oxidation. The chemistry is simulated using the REPROBUS (REactive Processes Ruling the Ozone BUdget in the Stratosphere) chemistry module that includes 55 chemical species and a comprehensive description of the stratospheric chemistry (Marchand et al., 2012; Lefèvre et al., 1994, 1998).

For Exp2a, the H_2O and SO_2 are injected at 27.5 km altitude using a Gaussian distribution and standard deviation of 2.5 km. The injection latitude ranges from 22 to 14° S, and longitude ranges from 182 to 186° E. The injections of H_2O and SO_2 are 150 and 0.5 Tg, respectively. The SSTs are taken from the IPSL climate-coupled simulation run under the CMIP6 Tier 1 SSP2-4.5 scenario (O'Neill et al., 2016).

4.10 MIROC-CHASER

The Model for Interdisciplinary Research On Climate – CHemical Atmospheric general circulation model for Study of atmospheric Environment and Radiative forcing (MIROC-CHASER) version 6 (Sekiya et al., 2016) is a chemistry climate model, with a top at around 0.004 hPa. The present version of MIROC-CHASER is built on MIROC6 (Tatebe et al., 2019) and has a spectral horizontal resolution of T85 (1.4° latitude × 1.4° longitude). The model has 81 vertical levels, with a vertical resolution 0.7 km in the lower stratosphere, ∼ 1.2 km in the upper stratosphere, and ∼ 3 km in the lower mesosphere. In the free-running simulations, the model generates QBO internally. The ensemble members have different initial conditions (1 January 2022), which are generated using slightly different nudging relaxation time during the spin-up. The aerosols are interactively simulated using a three-mode modal aerosol module (Seikiya et al., 2016). The chemistry uses comprehensive troposphere–stratosphere chemistry (Watanabe et al., 2011). The volcanic emission from continuously degassing volcanoes uses the emission inventory of Fioletov et al. (2022). For the explosive volcanic eruptions during the spin-up time, explosive volcanic emissions follow Carn (2022).

For Exp1 fixed-SST simulations, the model uses the observed SST from 10-year climatological mean from 2012 to 2021 using the monthly-1deg CMIP6 AMIP SST (Gates et al., 1999).

For Exp2a, the atmospheric temperature and winds are nudged to MERRA-2 reanalysis with a 12 h relaxation using 3 h meteorology. The observed SST uses the NOAA 1/4° Daily Optimum Interpolation Sea Surface Temperature (OISST) from 2022 to 2023 (Huang et al., 2020).

The initial volcanic injection altitude and area are not tuned but follow the experimental protocol. For Exp1 and Exp2a, the H_2O and SO_2 are injected at 25 to 30 km altitude. The injection latitude ranges from 22 to 14° S, and longitude ranges from 182 to 186° E. The initial injection of H_2O is 186 Tg, with ∼ 150 Tg left after the first week following the eruption. The large initial H_2O injection is necessary to keep 150 Tg in the stratosphere as requested by the experimental protocol because a large amount of ice clouds generates and falls to the troposphere soon after the eruption.

4.11 UKESM1.1

The United Kingdom Earth System Model (UKESM, Sellar et al., 2019, 2020) is the successor to the HadGEM2-ES model (Collins et al., 2011), jointly developed by the UK Met Office and the Natural Environment Research Council (NERC) to deliver simulations to the Coupled Model Intercomparison Project Phase 6 (CMIP6; Eyring et al., 2016). For HTHH-MOC, we run the updated UKESM1.1 system (Mulcahy et al., 2023), which consists of the physical climate model HadGEM3-GC3.1 (Kuhlbrodt et al., 2018; Williams et al., 2018) and has improved tropospheric aerosol processes and aerosol radiative forcings (Mulcahy et al., 2018, 2020). The GC3.1 system comprises the GA7.1 global atmosphere model configuration (Walters et al., 2019), which uses the ENDGAME dynamics system (Wood et al., 2014), at a resolution of 1.875° longitude by 1.25° latitude, with 85 levels extending to 85 km. Specifically the simulations apply the UKESM1.1-AMIP academic community release job (at v12.1 of the Unified Model), as supported by the UK National Centre for Atmospheric Science.

The interactive atmospheric chemistry module UKCA (UK Chemistry and Aerosols) has a number of chemistry configurations, with UKESM1.0 for CMIP6 applying the combined stratosphere and troposphere chemistry (CheST) option (Archibald et al., 2020), essentially a combination of the stratosphere chemistry (Morgenstern et al., 2009) and tropospheric chemistry (O'Connor et al., 2014) UKCA schemes. The UKCA aerosol scheme is the GLOMAP-mode aerosol microphysics module (Mann et al., 2010, 2012; Bellouin et al., 2013), with UKESM1.0 including the initial set of adaptations to GLOMAP for simulating stratospheric aerosol (Dhomse et al., 2014). For all UKESM1.0 integrations for CMIP6, the system was applied with evaporation of sulfate aerosol de-activated, stratospheric aerosol properties enacted from the CMIP6-prescribed zonal mean dataset (Luo, 2017; Jörimann, 2025), but for the integrations here we have applied the system for interactive aerosol across the troposphere and stratosphere, enacting a Hunga emission of volcanic SO_2 following the 0.5 Tg at 25–30 km Tonga-MIP protocols (see Table 6).

For the improved UKESM1.1 version applied here, the other most relevant development, compared to UKESM1.0 used for CMIP6, is the interactive atmospheric chemistry module UKCA (UK Chemistry and Aerosols), which has the updates to heterogeneous chemistry added by Dennison et al. (2019), to represent reactions occurring on the surfaces of polar stratospheric clouds and sulfate aerosol more realistically, with modified uptake coefficients of the five existing reactions and the addition of a further eight reactions involving bromine species. For these simulations, for the first time we have added the equilibrium liquid PSC scheme of Carslaw et al. (1995) to UKESM; this scheme is an interim implementation here coupling the five existing heterogeneous reactions of chlorine activation here then occurring on solid and now also liquid ternary-aerosol PSCs.

For Exp2, UKESM1.1 is run in a specified dynamics configuration (Telford et al., 2008, 2009), the atmospheric temperature and winds nudged to ERA5 every 6 h, the Newton relaxation applied for levels 12 to 80 of 85 (between 1 and 60 km). Sea-surface temperatures and sea ice are prescribed from the Reynolds v2.1 datasets, during both the 2017 to 2022 spin-up period and the 2-year Exp2 period to December 2023. Monthly varying anthropogenic atmospheric chemistry and aerosol emissions were set following the CMIP6 SSP2-4.5 datasets.

4.12 WACCM6/MAM4

The Whole Atmosphere Community Climate Model version 6 (WACCM6; Gettelman et al., 2019) is the high-top version of the atmospheric component of the Community Earth System Model, version 2 (CESM2), with a top at around 140 km. WACCM6 has a horizontal resolution of 0.9° latitude × 1.25° longitude, utilizing the finite-volume dynamical core (Lin and Rood, 1996). The model has 70 vertical levels, with a vertical resolution of ∼ 1 km in the lower stratosphere, ∼ 1.75 km in the upper stratosphere, and ∼ 3.5 km in the upper mesosphere and lower thermosphere (Garcia et al., 2017). In the free-running simulations, the model generates QBO internally (Mills et al., 2017; Gettelman et al., 2019). The ensemble members differ in the last date of nudging (from 27 January to 5 February 2022). The aerosol is interactively simulated using a four-mode modal aerosol module (MAM4; Liu et al., 2012, 2016; Mills et al., 2016), in which we used the Vehkamäki nucleation scheme (Vehkamäki et al., 2002). The chemistry uses comprehensive troposphere–stratosphere–mesosphere–lower thermosphere (TSMLT) chemistry (Gettelman et al., 2019). The volcanic emissions from continuously degassing volcanoes use the emission inventory of Andres and Kasgnoc (1998). For the explosive volcanic eruptions during the spin-up time, explosive volcanic emissions follow Mills et al. (2016) and Neely and Schmidt (2016), with updates until 2022.

For Exp1_CoupledOcean simulations, the ocean and sea ice are initialized on 3 January 2022 with output from a standalone ocean model forced by atmospheric state fields and fluxes from the Japanese 55-year Reanalysis (Tsujino et al., 2018). To accurately simulate the early plume structure and evolution, the winds and temperatures in WACCM are nudged toward the Analysis for Research and Applications, MERRA-2 meteorological data (Gelaro et al., 2017) throughout January 2022. After 1 February 2022, the model is free-running to capture fully coupled variability. For the fixed-SST simulation, the model uses the 10-year climatology SST from 2012 to 2021. The SST data are OISSTv2, which is a NOAA High-resolution (0.25 × 0.25) Blended Analysis of Daily SST and Ice (Banzon et al., 2022).

For Exp2, the atmospheric temperature and winds are nudged to MERRA-2 reanalysis with a 12 h relaxation using 3 h meteorology (Davis et al., 2022). The observed SST uses the 10-year climatological mean from 2012 to 2021.

The initial volcanic injection altitude and area are the same as described for Sect. 4.1 CAM5/CARMA.

4.13 WACCM6/CARMA

WACCM6/CARMA only performed Exp2 and used a configuration similar to WACCM6/MAM4 with the same horizontal and vertical resolution, SSTs, and meteorological nudging. Differences compared to WACCM6/MAM4 are the chemistry and aerosol configuration used. WACCM6/CARMA used the middle atmosphere chemistry with limited chemistry in the troposphere and comprehensive chemistry in the stratosphere, mesosphere, and lower thermosphere (Davis et al., 2022). Furthermore, we use the Community Aerosol and Radiation Model for Atmospheres (CARMA, Tilmes et al., 2023, based on Yu et al., 2015 with some updates) as the aerosol module, in which we used the Vehkamäki nucleation scheme (Vehkamäki et al., 2002). CARMA defines 20 mass bins and tracks the dry mass of the particles and assumes particle water is in equilibrium with the environmental water vapor. The approximate radius ranges from 0.2 nm to 1.3 µm in radius for the pure sulfate group that sulfate homogeneous nucleation occurs in and ranges from 0.05 to 8.7 µm in the mixed group that tracks all major tropospheric aerosol types (i.e., black carbon, organic carbon, sea salt, dust, sulfate).

The initial volcanic injection altitude and area are determined by validating the water and aerosol transportation in the first 6 months against MLS and OMPS observations. In these simulations, the H_2O is injected to 25 to 35 km altitude following Zhu et al. (2022), while the SO_2 is injected 82 % of the total mass to 26.5–28 km and 18 % to 28–36 km altitude. The injection latitude ranges from 22 to 6° S, and longitude ranges from 182.5 to 202.5° E.

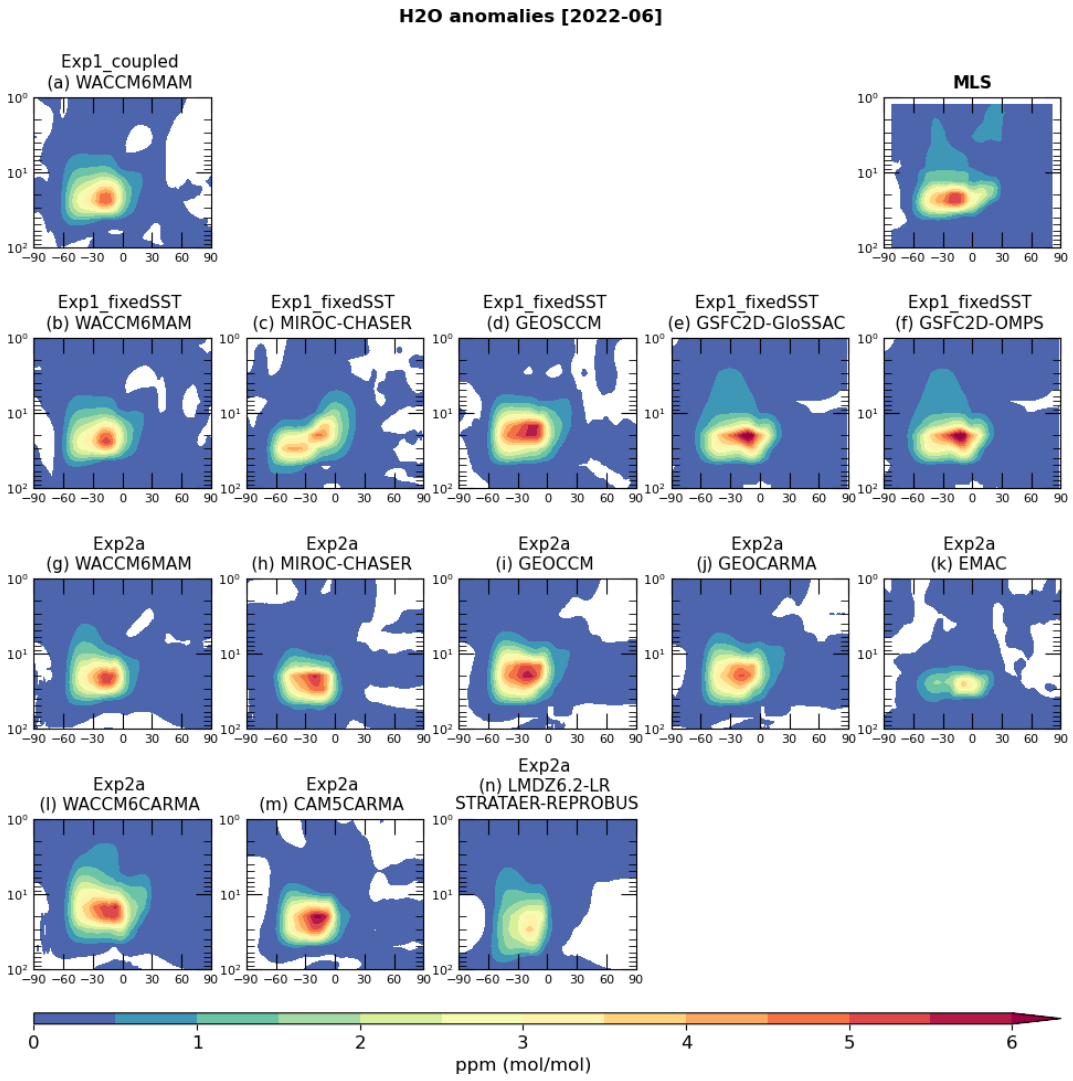

Figure 5. The zonal average H_2O anomaly in June 2022 from MLS, Exp1_fixedSST, Exp1_CoupledOcean, and Exp2a. The simulated anomaly is using the $H_2O + SO_2$ run minus the control run. And the MLS uses the 2022 data minus the climatology.

5 Preliminary results

The models' performances will be evaluated focusing on the following aspects: the stratospheric aerosol optical depth will be compared with GloSSAC and other satellite instruments individually such as OMPS-LP, SAGEIII-ISS, and OSIRIS; the aerosol effective radius will be compared with balloon observations (Asher et al., 2023), SAGEIII-ISS-retrieved size distribution, and AeroNet-retrieved particle radius; the water vapor lifetime, ozone, and its related chemicals (such as HCl, HNO_3, ClO) will be compared with MLS observations; and the temperature anomaly will be compared with the MLS detrended temperature field (Randel et al., 2024). All the evaluations will be conducted before looking into the climate impact of this eruption, such as radiative impact and tropospheric responses. This work will be described in a follow-up paper.

As the time of writing, we are still completing the model output inspection and validation phase. So, we can only provide preliminary results from some models. Figure 5 shows the preliminary results from Exp1 and Exp2 in June 2022 compared with the MLS v5 water vapor anomaly. The model results shown here generally agree with the MLS anomaly regarding the vertical (10–50 hPa) and horizontal distribution (60° S to 20° N) and the anomaly peaking at $\sim$6 ppmv for most of the models. This consistency of water vapor anomaly 6 months after the eruption helps us have confidence in these models for the analysis of climate and chemistry impacts and will be evaluated in detail in the follow up studies.

6 Summary

A multi-model observation comparison project is designed to evaluate the impact of the 2022 Hunga eruption. Two experiments are designed to cover various research interests for this eruption, including sulfate and water plume dispersion and transport, dynamical and chemical responses in the stratosphere, and climate impact. The project will not only benefit the Hunga Impact assessment but also benchmark the model performance in simulating stratospheric explosive volcanic eruption events and stratospheric water vapor injections. These events have a potentially large impact on the Earth system, especially on the stratospheric ozone layer and radiative balance.

Code and data availability. The data used to produce the results used in this paper are archived on Zenodo:

- https://doi.org/10.5281/zenodo.14962954 (Wang, 2025),
- https://doi.org/10.5281/zenodo.14963276 (Quaglia et al., 2025),
- https://doi.org/10.5281/zenodo.14961868 (Jörimann, 2025),
- https://doi.org/10.5281/zenodo.14962925 (Brühl, 2025).

Supplement. The supplement related to this article is available online at https://doi.org/10.5194/gmd-18-5487-2025-supplement.

Author contributions. YZ: concept design, project administration, experiment design, data archive, WACCM model setup. EA: NOAA balloon aerosol and water vapor observations for experiments. EB, ST, and JZ: experiment design and experiments using WACCM6MAM. AB: experiment design, data archive. AJ: experiment 2b-prescribed field preparation. MK: GloSSAC data for Exp 2b. TS and SW: SW conducted all MIROC-CHASER experiments, data post-processing, and data archive under supervision of TS, who developed the aerosol microphysics scheme of the model. XW and WY: experiment using WACCM6MAM. ZZ: experiment using WACCM6MAM, WACCM6MAM data post-processing, data archive. NL and SB: experiment using IPSL7-STRATAER, data post-processing, and archive. MM and LF: experiment using IPSL7-STRATAER-REPROBUS, data post-processing, and archive. SR and SC: experiments using IFS-COMPO. MC: experiment design, Tonga-MIP lead. FFØ, GK, and OM: experiment design. CB: experiment using EMAC. IQ, VA, RU, and AK: model output inspection and evaluation. EF: experiments using GSFC2D, data post-processing, and data archive. DP: experiment design and experiments using CMAM and data post-processing. PRC, LDO, QL, MM, and SS: experiment design and conducted experiments with the NASA GEOS CCM. PC and PRC: experiment design and experiments with the NASA GEOS CARMA model. HA and YY: experiment using CCSRNIES-MIROC3.2, data post-processing, and archive. DV: experiment design and assistance of EB with variables' request. WR and PN: concept design. GM: concept design and responsibility for JASMIN data archiving. PY and YP: experiments using CAM5CARMA and data post-processing. ST and C-CL: experiments using WACCM6CARMA and data post-processing.

Competing interests. At least one of the (co-)authors is a member of the editorial board of *Geoscientific Model Development*. The peer-review process was guided by an independent editor, and the authors also have no other competing interests to declare.

Disclaimer. Publisher's note: Copernicus Publications remains neutral with regard to jurisdictional claims made in the text, published maps, institutional affiliations, or any other geographical representation in this paper. While Copernicus Publications makes every effort to include appropriate place names, the final responsibility lies with the authors.

Acknowledgements. We acknowledge Michelle Santee, Martyn Chipperfield, Allegra Legrande, Thomas Peter, and Myriam Khodri for their valuable input for this project.

We acknowledge the APARC for their funding and other support of this activity.

This research has been supported by the National Oceanic and Atmospheric Administration (grant nos. 03-01-07-001, NA17OAR4320101, and NA22OAR4320151). NCAR's Community Earth System Model project is supported by the National Center for Atmospheric Research, which is a major facility sponsored by the NSF under cooperative agreement no. 1852977. Wandi Yu's work was performed under the auspices of the U.S. Department of Energy by Lawrence Livermore National Laboratory under Contract DE-AC52-07NA27344. Takashi Sekiya and Shingo Watanabe were supported by the MEXT-Program for The Advanced Studies of Climate Change Projection (SENTAN) (grant number JPMXD0722681344), and their MIROC-CHASER and MIROC-ES2H simulations were conducted using the Earth Simulator at JAMSTEC. IFS-Compo is supported by the Copernicus Atmosphere Monitoring Service (CAMS), which is one of six services that form Copernicus, the European Union's Earth observation program.

The IPSLCM7 model experiments were performed using the high-performance computing (HPC) resources of TGCC (Très Grand Centre de Calcul) under allocation 2024-A0170102201 (project gen2201) provided by GENCI (Grand Équipement National de Calcul Intensif). This study benefited from the ESPRI (Ensemble de Services Pour la Recherche l'IPSL) computing and data center (https://mesocentre.ipsl.fr, last access: 12 August 2025), which is supported by CNRS, Sorbonne Université, École Polytechnique, and CNES.

Valentina Aquila is supported by the NASA NNH22ZDA001N-ACMAP and NNH19ZDA001N-IDS programs.

Freja F. Østerstrøm acknowledges support from the European Union's Horizon 2020 research and innovation program under the Marie Skłodowska-Curie grant no. 891186.

Rei Ueyama is supported by NASA Upper Atmospheric Composition Observations and Aura Science Team programs as well as through the NASA Internal Scientist Funding Model.

Peter R. Colarco, Luke D. Oman, Qing Liang, Stephen Steenrod, Marion Marchand, and Parker Case are supported by the NASA

Modeling Analysis and Prediction program (program manager: David Considine, NASA HQ) through the NASA Internal Scientist Funding Model. Parker Case is additionally supported by the NASA Postdoctoral Program. GEOS CCM and GEOS CARMA simulations were performed at the NASA Center for Climate Simulation.

Hideharu Akiyoshi and Yousuke Yamashita were supported by KAKENHI (JP24K00700 and JP24H00751) of the Ministry of Education, Culture, Sports, Science, and Technology, Japan, and the NEC SX-AURORA TSUBASA platform at NIES was used to perform CCSRNIES-MIROC3.2 simulations.

Gabriel Chiodo acknowledges funding from the European Commission via the ERC StG 101078127 and the Spanish Ministry of Science and Innovation via the Ramon y Cajal grant no. RYC2021-033422-I.

We acknowledge funding from the UK National Centre for Atmospheric Science (NCAS) for Graham Mann and Sandip Dhomse via the NERC multi-centre Long-Term Science program on the North Atlantic climate system (ACSIS, NERC grant NE/N018001/1.

Andrin Jörimann acknowledges support from the Swiss National Science Foundation (SNSF) project AEON (grant no. 200020E_219166), as well as the partial support received by the SPARC Hunga Tonga aerosol forcing dataset activity. We are grateful to the UK Centre for Environmental Data Archiving (CEDA) for providing project group workspace and other modelling support within the UK collaborative "Joint Analysis System Meeting Infrastructure Needs" system (JASMIN, Lawrence et al., 2012).

Financial support. This research has been supported by the National Oceanic and Atmospheric Administration (grant nos. 03-01-07-001, NA17OAR4320101, and NA22OAR4320151); the National Science Foundation (grant no. 1852977); the Lawrence Livermore National Laboratory (grant no. DE-AC52-07NA27344); the Ministry of Education, Culture, Sports, Science and Technology (grant nos. JPMXD0722681344, JP24K00700, and JP24H00751); the National Aeronautics and Space Administration (grant nos. NNH22ZDA001N-ACMAP and NNH19ZDA001N-IDS); and the H2020 Marie Skłodowska-Curie Actions (grant no. 891186). Graham W. Mann and Sandip S. Dhomse were part-funded also by the Natural Environment Research Council (NERC) standard grant project MeteorStrat (grant no. NE/R011222/1). The UKESM1.1 HTHH-MOC simulations were carried out on the joint UK Met Office and Natural Environment Research Council (NERC) MONSooN supercomputing system ("Met Office and NERC Supercomputer Nodes").

Review statement. This paper was edited by Lele Shu and reviewed by Jean-Francois Lamarque, Shuaiqi Wu, and Bjoern-Martin Sinnhuber.

References

Akiyoshi, H., Nakamura, T., Miyasaka, T., Shiotani, M., and Suzuki, M.: A nudged chemistry-climate model simulation of chemical constituent distribution at northern high-latitude stratosphere observed by SMILES and MLS during the 2009/2010 stratospheric sudden warming, J. Geophys. Res.-Atmos., 121, 1361–1380, https://doi.org/10.1002/2015JD023334, 2016.

Akiyoshi, H., Kadowaki, M., Yamashita, Y., and Nagatomo, T.: Dependence of column ozone on future ODSs and GHGs in the variability of 500-ensemble members, Sci. Rep., 13, 320, https://doi.org/10.1038/s41598-023-27635-y, 2023.

Andres, R. J. and Kasgnoc, A. D.: A time-averaged inventory of subaerial volcanic sulfur emissions, J. Geophys. Res., 103, 25251–25261, https://doi.org/10.1029/98JD02091, 1998.

Archibald, A. T., O'Connor, F. M., Abraham, N. L., Archer-Nicholls, S., Chipperfield, M. P., Dalvi, M., Folberth, G. A., Dennison, F., Dhomse, S. S., Griffiths, P. T., Hardacre, C., Hewitt, A. J., Hill, R. S., Johnson, C. E., Keeble, J., Köhler, M. O., Morgenstern, O., Mulcahy, J. P., Ordóñez, C., Pope, R. J., Rumbold, S. T., Russo, M. R., Savage, N. H., Sellar, A., Stringer, M., Turnock, S. T., Wild, O., and Zeng, G.: Description and evaluation of the UKCA stratosphere–troposphere chemistry scheme (StratTrop vn 1.0) implemented in UKESM1, Geosci. Model Dev., 13, 1223–1266, https://doi.org/10.5194/gmd-13-1223-2020, 2020.

Asher, E., Todt, M., Rosenlof, K., Thornberry, T., Gao, R., Taha, G., Walter, P., Alvarez, S., Flynn, J., Davis, S. M., Evan, S., Brioude, J., Metzger, J., Hurst, D. F., Hall, E., and Xiong, K.: Unexpectedly rapid aerosol formation in the Hunga Tonga plume, P. Natl. Acad. Sci. USA, 120, e2219547120, https://doi.org/10.1073/pnas.2219547120, 2023.

Bacmeister, J. T., Schoeberl, M. R., Summers, M. E., Rosenfield, J. E., and Zhu, X.: Descent of long-lived trace gases in the winter polar vortex. J. Geophys. Res., 100, 11669–11684, https://doi.org/10.1029/94jd02958, 1995.

Bacmeister, J. T., Suarez, M. J., and Robertson, F. R.: Rain reevaporation, boundary layer–convection interactions, and Pacific rainfall patterns in an AGCM, J. Atmos. Sci., 63, 3383–3403, 2006.

Banzon, V., Reynolds, R., and National Center for Atmospheric Research Staff (Eds.): Last modified 2022-09-09 "The Climate Data Guide: SST data: NOAA High-resolution (0.25×0.25) Blended Analysis of Daily SST and Ice, OISSTv2", https://climatedataguide.ucar.edu/climate-data/sst-data-noaa-high-resolution-025x025-blended-analysis-daily-sst-and-ice-oisstv2 (last access: 4 February 2025), 2022.

Bellouin, N., Mann, G. W., Woodhouse, M. T., Johnson, C., Carslaw, K. S., and Dalvi, M.: Impact of the modal aerosol scheme GLOMAP-mode on aerosol forcing in the Hadley Centre Global Environmental Model, Atmos. Chem. Phys., 13, 3027–3044, https://doi.org/10.5194/acp-13-3027-2013, 2013.

Bernath, P. F., McElroy, C. T., Abrams, M. C., Boone, C. D., Butler, M., Camy-Peyret, C., Carleer, M., Clerbaux, C., Coheur, P.-F., Colin, R., DeCola, P., DeMazière, M., Drummond, J. R., Dufour, D., Evans, W. F. J., Fast, H., Fussen, D., Gilbert, K., Jennings, D. E., Llewellyn, E. J., Lowe, R. P., Mahieu, E., McConnell, J. C., McHugh, M., McLeod, S. D., Michaud, R., Midwinter, C., Nassar, R., Nichitiu, F., Nowlan, C., Rinsland, C. P., Rochon, Y. J., Rowlands, N., Semeniuk, K., Simon, P., Skelton, R., Sloan, J. J., Soucy, M.-A., Strong, K., Tremblay, P., Turnbull, D., Walker, K. A., Walkty, I., Wardle, D. A., Wehrle, V., Zander, R., and Zou, J., Atmospheric Chemistry Experiment (ACE): Mission overview, Geophys. Res. Lett., 32, L15S01, https://doi.org/10.1029/2005GL022386, 2005.

Boucher, O., Servonnat, J., Albright, A. L., Aumont, O., Balkanski, Y., Bastrikov, V., Bekki, S., Bonnet, R., Bony, S., Bopp, L., Bra-

connot, P., Brockmann, P., Cadule, P., Caubel, A., Cheruy, F., Codron, F., Cozic, A., Cugnet, D., D'Andrea, F., Davini, P., de Lavergne, C., Denvil, S., Deshayes, J., Devilliers, M., Ducharne, A., Dufresne, J.-L., Dupont, E., Éthé, C., Fairhead, L., Falletti, L., Flavoni, S., Foujols, M.-A., Gardoll,S., Gastineau, G., Ghattas, J., Grandpeix, J.-Y. Guenet, B., Lionel, E. Guez, Guilyardi, E., Guimberteau, M., Hauglustaine, D., Hourdin, F., Idelkadi, A., Joussaume, S., Kageyama, M., Khodri, M., Krinner, G., Lebas, N., Levavasseur, G., Lévy, C., Li, L., Lott, F., Lurton, T., Luyssaert, S., Madec, G., Madeleine, J.-B., Maignan, F., Marchand, M., Marti, O., Mellul, L., Meurdesoif, Y., Mignot, J., Musat, I., Ottlé, C., Peylin, P., Planton, Y., Polcher, I., Rio, C., Rochetin, N., Rousset, C., Sepulchre, P., Sima, A., Swingedouw, D., Thiéblemont, R., Traore, A. K., Vancoppenolle, M., Vial, J., Vialard, J., Viovy, N., and Vuichard, N.: Presentation and evaluation of the IPSL-CM6A-LR climate model, J. Adv. Model. Earth Sy., 12, e2019MS002010, https://doi.org/10.1029/2019MS002010, 2020.

Bretherton, C. S. and Park, S.: A new moist turbulence parameterization in the Community Atmosphere Model, J. Climate, 22, 3422–3448, 2009.

Brodowsky, C., Sukhodolov, T., Feinberg, A., Höpfner, M., Peter, T., Stenke, A., and Rozanov, E.: Modeling the sulfate aerosol evolution after recent moderate volcanic activity, 2008–2012, J. Geophys. Res.-Atmos., 126, e2021JD035472, https://doi.org/10.1029/2021JD035472, 2021.

Bruehl, C., Lelieveld, J., Schallock, J., and Rieger, L. A.: Chemistry Climate Model Studies on the Effect of the Hunga Tonga Eruption on stratospheric Ozone in mid and high Latitudes in 2022, in: AGU Fall Meeting Abstracts, Vol. 2023, No. 2235, A21B–2235, https://doi.org/2023AGUFM.A21B2235B, 2023.

Brühl, C.: SO_2 emission for EMAC MPIC model, Zenodo [data set], https://doi.org/10.5281/zenodo.14962925, 2025.

Carn, S.: Multi-Satellite Volcanic Sulfur Dioxide L4 Long-Term Global Database V4, Greenbelt, MD, USA, Goddard Earth Science Data and Information Services Center (GES DISC), https://doi.org/10.5067/MEASURES/SO2/DATA405, 2022.

Carn, S., Clarisse, L., and Prata, A.: Multi-decadal satellite measurements of global volcanic degassing, J. Volcanol. Geoth. Res., 311, 99–134, https://doi.org/10.1016/j.jvolgeores.2016.01.002, 2016.

Carn, S., Fioletov, V., McLinden, C., Li, C., and Krotkov, N. A.: A decade of global volcanic SO_2 emissions measured from space, Sci. Rep., 7, 44095, https://doi.org/10.1038/srep44095, 2017.

Carn, S. A., Krotkov, N. A., Fisher, B. L., and Li, C.: Out of the blue: Volcanic SO_2 emissions during the 2021–2022 eruptions of Hunga Tonga–Hunga Ha'apai (Tonga), Frontiers in Earth Science, 10, 976962, https://doi.org/10.3389/feart.2022.976962, 2022.

Carslaw, K. S., Luo, B., and Peter, T.: An analytic expression for the composition of aqueous HNO_3-H_2SO_4 Stratospheric aerosols including gas phase removal of HNO_3, Geophys. Res. Lett., 22, 1877–1880, https://doi.org/10.1029/95GL01668, 1995.

Case, P., Colarco, P. R., Toon, B., Aquila, V., and Keller, C. A.: Interactive stratospheric aerosol microphysics-chemistry simulations of the 1991 Pinatubo volcanic aerosols with newly coupled sectional aerosol and stratosphere-troposphere chemistry modules in the NASA GEOS Chemistry-Climate Model (CCM), J. Adv. Model. Earth Sy., 15, e2022MS003147, https://doi.org/10.1029/2022MS003147,2023.

Clyne, M.: Modeling the Role of Volcanoes in the Climate System – Chapter 4: Tonga-MIP, PhD dissertation, University of Colorado at Boulder, ProQuest Dissertations & Theses, 31487034, 153 pp., 2024.

Collins, W. J., Bellouin, N., Doutriaux-Boucher, M., Gedney, N., Halloran, P., Hinton, T., Hughes, J., Jones, C. D., Joshi, M., Liddicoat, S., Martin, G., O'Connor, F., Rae, J., Senior, C., Sitch, S., Totterdell, I., Wiltshire, A., and Woodward, S.: Development and evaluation of an Earth-System model – HadGEM2, Geosci. Model Dev., 4, 1051–1075, https://doi.org/10.5194/gmd-4-1051-2011, 2011.

Collow, A. B., Colarco, P. R., da Silva, A. M., Buchard, V., Bian, H., Chin, M., Das, S., Govindaraju, R., Kim, D., and Aquila, V.: Benchmarking GOCART-2G in the Goddard Earth Observing System (GEOS), Geosci. Model Dev., 17, 1443–1468, https://doi.org/10.5194/gmd-17-1443-2024, 2024.

Davis, N. A., Callaghan, P., Simpson, I. R., and Tilmes, S.: Specified dynamics scheme impacts on wave-mean flow dynamics, convection, and tracer transport in CESM2 (WACCM6), Atmos. Chem. Phys., 22, 197–214, https://doi.org/10.5194/acp-22-197-2022, 2022.

Dennison, F., Keeble, J., Morgenstern, O., Zeng, G., Abraham, N. L., and Yang, X.: Improvements to stratospheric chemistry scheme in the UM-UKCA (v10.7) model: solar cycle and heterogeneous reactions, Geosci. Model Dev., 12, 1227–1239, https://doi.org/10.5194/gmd-12-1227-2019, 2019.

Dhomse, S. S., Emmerson, K. M., Mann, G. W., Bellouin, N., Carslaw, K. S., Chipperfield, M. P., Hommel, R., Abraham, N. L., Telford, P., Braesicke, P., Dalvi, M., Johnson, C. E., O'Connor, F., Morgenstern, O., Pyle, J. A., Deshler, T., Zawodny, J. M., and Thomason, L. W.: Aerosol microphysics simulations of the Mt. Pinatubo eruption with the UM-UKCA composition-climate model, Atmos. Chem. Phys., 14, 11221–11246, https://doi.org/10.5194/acp-14-11221-2014, 2014.

Dhomse, S. S., Mann, G. W., Antuña Marrero, J. C., Shallcross, S. E., Chipperfield, M. P., Carslaw, K. S., Marshall, L., Abraham, N. L., and Johnson, C. E.: Evaluating the simulated radiative forcings, aerosol properties, and stratospheric warmings from the 1963 Mt Agung, 1982 El Chichón, and 1991 Mt Pinatubo volcanic aerosol clouds, Atmos. Chem. Phys., 20, 13627–13654, https://doi.org/10.5194/acp-20-13627-2020, 2020.

Duncan, B. N., Logan, J. A., Bey, I., Megretskaia, I. A., Yantosca, R. M., Novelli, P. C., Jones, N. B., and Rinsland, C. P.: Global budget of CO, 1988–1997: Source estimates and validation with a global model, J. Geophys. Res.-Atmos., 112, D22301, https://doi.org/10.1029/2007JD008459, 2007.

Emmons, L. K., Walters, S., Hess, P. G., Lamarque, J.-F., Pfister, G. G., Fillmore, D., Granier, C., Guenther, A., Kinnison, D., Laepple, T., Orlando, J., Tie, X., Tyndall, G., Wiedinmyer, C., Baughcum, S. L., and Kloster, S.: Description and evaluation of the Model for Ozone and Related chemical Tracers, version 4 (MOZART-4), Geosci. Model Dev., 3, 43–67, https://doi.org/10.5194/gmd-3-43-2010, 2010.

English, J. M., Toon, O. B., Mills, M. J., and Yu, F.: Microphysical simulations of new particle formation in the upper troposphere and lower stratosphere, Atmos. Chem. Phys., 11, 9303–9322, https://doi.org/10.5194/acp-11-9303-2011, 2011.

English, J. M., Toon, O. B., and Mills, M. J.: Microphysical simulations of large volcanic eruptions: Pinatubo and Toba, J. Geophys. Res.-Atmos., 118, 1880–1895, 2013.

Errera, Q., Chabrillat, S., Christophe, Y., Debosscher, J., Hubert, D., Lahoz, W., Santee, M. L., Shiotani, M., Skachko, S., von Clarmann, T., and Walker, K.: Technical note: Reanalysis of Aura MLS chemical observations, Atmos. Chem. Phys., 19, 13647–13679, https://doi.org/10.5194/acp-19-13647-2019, 2019.

Eskes, H., Tsikerdekis, A., Ades, M., Alexe, M., Benedictow, A. C., Bennouna, Y., Blake, L., Bouarar, I., Chabrillat, S., Engelen, R., Errera, Q., Flemming, J., Garrigues, S., Griesfeller, J., Huijnen, V., Ilić, L., Inness, A., Kapsomenakis, J., Kipling, Z., Langerock, B., Mortier, A., Parrington, M., Pison, I., Pitkänen, M., Remy, S., Richter, A., Schoenhardt, A., Schulz, M., Thouret, V., Warneke, T., Zerefos, C., and Peuch, V.-H.: Technical note: Evaluation of the Copernicus Atmosphere Monitoring Service Cy48R1 upgrade of June 2023, Atmos. Chem. Phys., 24, 9475–9514, https://doi.org/10.5194/acp-24-9475-2024, 2024.

Eyring, V., Cionni, I., Bodeker, G. E., Charlton-Perez, A. J., Kinnison, D. E., Scinocca, J. F., Waugh, D. W., Akiyoshi, H., Bekki, S., Chipperfield, M. P., Dameris, M., Dhomse, S., Frith, S. M., Garny, H., Gettelman, A., Kubin, A., Langematz, U., Mancini, E., Marchand, M., Nakamura, T., Oman, L. D., Pawson, S., Pitari, G., Plummer, D. A., Rozanov, E., Shepherd, T. G., Shibata, K., Tian, W., Braesicke, P., Hardiman, S. C., Lamarque, J. F., Morgenstern, O., Pyle, J. A., Smale, D., and Yamashita, Y.: Multi-model assessment of stratospheric ozone return dates and ozone recovery in CCMVal-2 models, Atmos. Chem. Phys., 10, 9451–9472, https://doi.org/10.5194/acp-10-9451-2010, 2010.

Eyring, V., Lamarque, J.-F., Hess, P., Arfeuille, F., Bowman, K., Chipperfield, M. P., Duncan, B., Fiore, A., Gettelman, A., Giorgetta, M. A., Granier, C., Hegglin, M., Kinnison, D., Kunze, M., Langematz, U., Luo, B., Martin, R., Matthes, K., Newman, P.A., Peter, T., Robock, A., Ryerson, T., Saiz-Lopez, A., Salawitch, R., Schultz, M., Shepherd, T.G., Shindell, D., Staehelin, J., Tegtmeier, S., Thomason, L., Tilmes, S., Vernier, J.-P., Waugh, D. W., and Young, P. J.: Overview of the IGAC/SPARC Chemistry-Climate Model Initiative (CCMI) Community Simulations in Support of Upcoming Ozone and Climate Assessments, SPARC newsletter no. 40, http://www.aparc-climate.org/wp-content/uploads/2017/12/SPARCnewsletter_No40_Jan2013_web.pdf (last access: 21 August 2025), 2013.

Eyring, V., Bony, S., Meehl, G. A., Senior, C. A., Stevens, B., Stouffer, R. J., and Taylor, K. E.: Overview of the Coupled Model Intercomparison Project Phase 6 (CMIP6) experimental design and organization, Geosci. Model Dev., 9, 1937–1958, https://doi.org/10.5194/gmd-9-1937-2016, 2016.

Fioletov, V., McLinden, C. A., Griffin, D., Abboud, I., Krotkov, N., Leonard, P. J. T., Li, C., Joiner, J., Theys, N., and Carn, S.: Multi-Satellite Air Quality Sulfur Dioxide (SO_2) Database Long-Term L4 Global V2, Edited by Peter Leonard, Greenbelt, MD, USA, Goddard Earth Science Data and Information Services Center (GES DISC) [data set], https://doi.org/10.5067/MEASURES/SO2/DATA406, 2022.

Fleming, E. L., Newman, P. A., Liang, Q., and Daniel, J. S.: The impact of continuing CFC-11 emissions on stratospheric ozone, J. Geophys. Res.-Atmos., 125, e2019JD031849, https://doi.org/10.1029/2019jd031849, 2020.

Fleming, E. L., Newman, P. A., Liang, Q., and Oman, L. D.: Stratospheric temperature and ozone impacts of the Hunga Tonga-Hunga Ha'apai water vapor injection, J. Geophys. Res.-Atmos., 129, e2023JD039298, https://doi.org/10.1029/2023JD039298, 2024.

Flemming, J., Huijnen, V., Arteta, J., Bechtold, P., Beljaars, A., Blechschmidt, A.-M., Diamantakis, M., Engelen, R. J., Gaudel, A., Inness, A., Jones, L., Josse, B., Katragkou, E., Marecal, V., Peuch, V.-H., Richter, A., Schultz, M. G., Stein, O., and Tsikerdekis, A.: Tropospheric chemistry in the Integrated Forecasting System of ECMWF, Geosci. Model Dev., 8, 975–1003, https://doi.org/10.5194/gmd-8-975-2015, 2015.

Fomichev, V. I., Fu, C., de Grandpre, J., Beagley, S. R., Ogibalov, V. P., and McConnell, J. C.: Model thermal response to minor radiative energy sources and sinks in the middle atmosphere, J. Geophys. Res., 109, D19107, https://doi.org/10.1029/2004JD004892, 2004.

Garcia, R. R., Smith, A. K., Kinnison, D. E., Cámara, Á. d. l., and Murphy, D. J.: Modification of the Gravity Wave Parameterization in the Whole Atmosphere Community Climate Model: Motivation and Results, J. Atmos. Sci., 74, 275–291, https://doi.org/10.1175/JAS-D-16-0104.1, 2017.

Gates, W. L., Boyle, J. S., Covey, C., Dease, C. G., Doutriaux, C. M., Drach, R. S., Fiorino, M., Gleckler, P. J., Hnilo, J. J., Marlais, S. M., Phillips, T. J., Potter, G. L., Santer, B. D., Sperber, K. R., Taylor, K. E., and Williams, D. N.: An Overview of the Results of the Atmospheric Model Intercomparison Project (AMIP I), B. Am. Meteorol. Soc., 80, 29–55, https://doi.org/10.1175/1520-0477(1999)080<0029:AOOTRO>2.0.CO;2, 1999.

Gelaro, R., McCarty, W., Suárez, M. J., Todling, R., Molod, A., Takacs, L., Randles, C. A., Darmenov, A., Bosilovich, M. G., Reichle, R., Wargan, K., Coy, L., Cullather, R., Draper, C., Akella, S., Buchard, V., Conaty, A., da Silva, A. M., Gu, W., Kim, G., Koster, R., Lucchesi, R., Merkova, D., Nielsen, J. E., Partyka, G., Pawson, S., Putman, W., Rienecker, M., Schubert, S. D., Sienkiewicz, M., and Zhao, B.: The Modern-Era Retrospective Analysis for Research and Applications, Version 2 (MERRA-2), J. Climate, 30, 5419–5454, https://doi.org/10.1175/JCLI-D-16-0758.1, 2017.

Gettelman, A., Mills, M. J., Kinnison, D. E., Garcia, R. R., Smith, A. K., Marsh, D. R., Tilmes, S., Vitt, F., Bardeen, C. G., McInerney, J., Liu, H.-L., Solomon, S. C., Polvani, L. M., Emmons, L. K., Lamarque, J.-F., Richter, J. H., Glanville, A. S., Bacmeister, J. T., Phillips, A. S., Neale, R. B., Simpson, I. R., DuVivier, A. K., Hodzic, A., and Randel, W. J.: The Whole Atmosphere Community Climate Model Version6 (WACCM6), J. Geophys. Res.-Atmos., 124, 12380–12403, https://doi.org/10.1029/2019JD030943, 2019.

Gidden, M. J., Riahi, K., Smith, S. J., Fujimori, S., Luderer, G., Kriegler, E., van Vuuren, D. P., van den Berg, M., Feng, L., Klein, D., Calvin, K., Doelman, J. C., Frank, S., Fricko, O., Harmsen, M., Hasegawa, T., Havlik, P., Hilaire, J., Hoesly, R., Horing, J., Popp, A., Stehfest, E., and Takahashi, K.: Global emissions pathways under different socioeconomic scenarios for use in CMIP6: a dataset of harmonized emissions trajectories through the end of the century, Geosci. Model Dev., 12, 1443–1475, https://doi.org/10.5194/gmd-12-1443-2019, 2019.

Giorgetta, M. A., Manzini, E., Roeckner, E., Esch, M., and Bengtsson, L.: Climatology and forcing of the quasi-biennial oscilla-

tion in the MAECHAM5 model, J. Climate, 19, 3882–3901, https://doi.org/10.1175/JCLI3830.1, 2006.

Grell, G. A. and Freitas, S. R.: A scale and aerosol aware stochastic convective parameterization for weather and air quality modeling, Atmos. Chem. Phys., 14, 5233–5250, https://doi.org/10.5194/acp-14-5233-2014, 2014.

Hersbach, H., Bell, B., Berrisford, P., Hirahara, S., Horányi, A., Muñoz-Sabater, J., Nicolas, J., Peubey, C., Radu, R., Schepers, D., Simmons, A., Soci, C., Abdalla, S., Abellan, X., Balsamo, G., Bechtold, P., Biavati, G., Bidlot, J., Bonavita, M., De Chiara, G., Dahlgren, P., Dee, D., Diamantakis, M., Dragani, R., Flemming, J., Forbes, R., Fuentes, M., Geer, A., Haimberger, L., Healy, S., Hogan, R.J., Hólm, E., Janisková, M., Keeley, S., Laloyaux, P., Lopez, P., Lupu, C., Radnoti, G., de Rosnay, P., Rozum, I., Vamborg, F., Villaume, S., and Thépaut, J.-N.: The ERA5 global reanalysis, Q. J. Roy. Meteor. Soc., 146, 1999–2049, https://doi.org/10.1002/qj.3803, 2020.

Hourdin, F., Musat, I., Bony, S., Braconnot, P., Codron, F., Dufresne, J.-L., Fairhead, L., Filiberti, M.-A., Friedlingstein, P., Grandpeix, J.-Y., Krinner, G., Levan, P., Li, Z.-X., and Lott, F.: The LMDZ4 general circulation model: climate performance and sensitivity to parametrized physics with emphasis on tropical convection, Clim. Dynam., 27, 787–813, 2006.

Huang, B., Liu, C., Banzon, V., Freeman, E., Graham, G., Hankins, B., Smith, T., and Zhang, H.-M.,: Improvements of the Daily Optimum Interpolation Sea Surface Temperature (DOISST) Version 2.1, J. Climate, 34, 2923–2939, https://doi.org/10.1175/JCLI-D-20-0166.1, 2020.

Huijnen, V., Flemming, J., Chabrillat, S., Errera, Q., Christophe, Y., Blechschmidt, A.-M., Richter, A., and Eskes, H.: C-IFS-CB05-BASCOE: stratospheric chemistry in the Integrated Forecasting System of ECMWF, Geosci. Model Dev., 9, 3071–3091, https://doi.org/10.5194/gmd-9-3071-2016, 2016.

Hurrell, J. W., Holland, M. M., Gent, P. R., Ghan, S., Kay, J. E., Kushner, P. J., Lamarque, J.-F., Large, W. G., Lawrence, D., Lindsay, K., Lipscomb, W. H., Long, M. C., Mahowald, N., Marsh, D. R., Neale, R. B., Rasch, P., Vavrus, S., Vertenstein, M., Bader, D., Collins, W. D., Hack, J. J., Kiehl, J., and Marshall, S.: The community Earth system model: A framework for collaborative research, B. Am. Meteorol. Soc., 94, 1339–1360, https://doi.org/10.1175/BAMS-D-12-00121.1, 2013.

Iacono, M. J., Delamere, J. S., Mlawer, E. J., Shephard, M. W., Clough, S. A., and Collins, W. D.: Radiative forcing by long-lived greenhouse gases: Calculations with the AER radiative transfer models, J. Geophys. Res.-Atmos., 113, D13103, https://doi.org/10.1029/2008JD009944, 2008.

Jöckel, P., Kerkweg, A., Pozzer, A., Sander, R., Tost, H., Riede, H., Baumgaertner, A., Gromov, S., and Kern, B.: Development cycle 2 of the Modular Earth Submodel System (MESSy2), Geosci. Model Dev., 3, 717–752, https://doi.org/10.5194/gmd-3-717-2010, 2010.

Jones, A. C., Haywood, J. M., Jones, A., and Aquila, V.: Sensitivity of volcanic aerosol dispersion to meteorological conditions: a Pinatubo case study, J. Geophys. Res., 121, 6892–6908, https://doi.org/10.1002/2016JD025001, 2016.

Jonsson, A. I., de Grandpré, J., Fomichev, V. I., McConnell, J. C., and Beagley, S. R.: Doubled CO_2-induced cooling in the middle atmosphere: Photochemical analysis of the ozone radiative feedback, J. Geophys. Res., 109, D24103, https://doi.org/10.1029/2004JD005093, 2004.

Jörimann, A.: REMAP-GloSSAC-2023, Version v1, Zenodo [data set], https://doi.org/10.5281/zenodo.14961868, 2025.

Kawamiya, M., Hajima, T., Tachiiri, K., Watanabe, S., and Yokohata T.: Two decades of Earth system modeling with an emphasis on Model for Interdisciplinary Research on Climate (MIROC), Prog. Earth Planet. Sc., 7, 64, https://doi.org/10.1186/s40645-020-00369-5, 2020.

Kleinschmitt, C., Boucher, O., Bekki, S., Lott, F., and Platt, U.: The Sectional Stratospheric Sulfate Aerosol module (S3A-v1) within the LMDZ general circulation model: description and evaluation against stratospheric aerosol observations, Geosci. Model Dev., 10, 3359–3378, https://doi.org/10.5194/gmd-10-3359-2017, 2017.

Kohl, M., Brühl, C., Schallock, J., Tost, H., Jöckel, P., Jost, A., Beirle, S., Höpfner, M., and Pozzer, A.: New submodel for emissions from Explosive Volcanic ERuptions (EVER v1.1) within the Modular Earth Submodel System (MESSy, version 2.55.1), Geosci. Model Dev., 18, 3985–4007, https://doi.org/10.5194/gmd-18-3985-2025, 2025.

Kovilakam, M., Thomason, L. W., Ernest, N., Rieger, L., Bourassa, A., and Millán, L.: The Global Space-based Stratospheric Aerosol Climatology (version 2.0): 1979–2018, Earth Syst. Sci. Data, 12, 2607–2634, https://doi.org/10.5194/essd-12-2607-2020, 2020.

Kovilakam, M., Thomason, L., and Knepp, T.: SAGE III/ISS aerosol/cloud categorization and its impact on GloSSAC, Atmos. Meas. Tech., 16, 2709–2731, https://doi.org/10.5194/amt-16-2709-2023, 2023.

Kuhlbrodt, T., Jones, C. G., Sellar, A., Storkey, D., Blockley, E., Stringer, M., Hill, R., Graham, T., Ridley, J., Blaker, A., Calvert, D., Copsey, D., Ellis, R., Hewitt, H., Hyder, P., Ineson, S., Mulcahy, J., Siahaan, A., and Walton, J.: The Low–Resolution Version of HadGEM3 GC3.1: Development and Evaluation for Global Climate, J. Adv. Model. Earth Sy., 10, 2865–2888, https://doi.org/10.1029/2018MS001370, 2018.

Lamarque, J.-F., Emmons, L. K., Hess, P. G., Kinnison, D. E., Tilmes, S., Vitt, F., Heald, C. L., Holland, E. A., Lauritzen, P. H., Neu, J., Orlando, J. J., Rasch, P. J., and Tyndall, G. K.: CAM-chem: description and evaluation of interactive atmospheric chemistry in the Community Earth System Model, Geosci. Model Dev., 5, 369–411, https://doi.org/10.5194/gmd-5-369-2012, 2012.

Lawrence, B. N., Bennett, V., Churchill, J., Juckes, M., Kershaw, P., Oliver, P., Pritchard, M., and Stephens, A.: The JASMIN super-data-cluster, arXiv [preprint], https://doi.org/10.48550/arXiv.1204.3553, 2012.

Lefèvre, F., Brasseur, G. P., Folkins, I., Smith, A. K., and Simon, P.: Chemistry of the 1991–1992 stratospheric winter: Three-dimensional model simulations, J. Geophys. Res.-Atmos., 99, 8183–8195, https://doi.org/10.1029/93JD03476, 1994.

Lefèvre, F., Figarol, F., Carslaw, K. S., and Peter, T.: The 1997 Arctic Ozone depletion quantified from three-dimensional model simulations, Geophys. Res. Lett., 25, 2425–2428, https://doi.org/10.1029/98GL51812, 1998.

Jörimann, A., Sukhodolov, T., Luo, B., Chiodo, G., Mann, G., and Peter, T.: A REtrieval Method for optical and physical

Aerosol Properties in the stratosphere (REMAPv1), EGUsphere [preprint], https://doi.org/10.5194/egusphere-2025-145, 2025.

Li, C., Peng, Y., Asher, E., Baron, A. A., Todt, M., Thornberry, T. D., Evan, S., Brioude, J., Smale, P., Querel, R., Rosenlof, K. H., Zhou, L., Xu, J., Qie, K., Bian, J., Toon, O. B., Zhu, Y., and Yu, P.: Microphysical simulation of the 2022 Hunga volcano eruption using a sectional aerosol model, Geophys. Res. Lett., 51, e2024GL108522, https://doi.org/10.1029/2024GL108522, 2024.

Lin, S. J. and Rood, R. B.: Multidimensional flux-form semi-Lagrangian transport schemes, Mon. Weather Rev., 124, 2046–2070, https://doi.org/10.1175/1520-0493(1996)124<2046:MFFSLT>2.0.CO;2, 1996.

Liu, X., Easter, R. C., Ghan, S. J., Zaveri, R., Rasch, P., Shi, X., Lamarque, J.-F., Gettelman, A., Morrison, H., Vitt, F., Conley, A., Park, S., Neale, R., Hannay, C., Ekman, A. M. L., Hess, P., Mahowald, N., Collins, W., Iacono, M. J., Bretherton, C. S., Flanner, M. G., and Mitchell, D.: Toward a minimal representation of aerosols in climate models: description and evaluation in the Community Atmosphere Model CAM5, Geosci. Model Dev., 5, 709–739, https://doi.org/10.5194/gmd-5-709-2012, 2012.

Liu, X., Ma, P.-L., Wang, H., Tilmes, S., Singh, B., Easter, R. C., Ghan, S. J., and Rasch, P. J.: Description and evaluation of a new four-mode version of the Modal Aerosol Module (MAM4) within version 5.3 of the Community Atmosphere Model, Geosci. Model Dev., 9, 505–522, https://doi.org/10.5194/gmd-9-505-2016, 2016.

Lock, A. P., Brown, A. R., Bush, M. R., Martin, G. M., and Smith, R. N. B.: A new boundary layer mixing scheme. Part I: Scheme description and single-column model tests, Mon. Weather Rev., 128, 3187–3199, 2000.

Luo, B.: SAGE-3λv4: Stratospheric aerosol data for use in CMIP6 models, ETH Zurich [data set], https://doi.org/10.3929/ethz-b-000715155, 2017.

Lurton, T., Balkanski, Y., Bastrikov, V., Bekki, S., Bopp, L., Braconnot, P., Brockmann, P., Cadule, P., Contoux, C., Cozic, A., Cugnet, D., Dufresne, J.-L., Éthé, C., Foujols, M.-A., Ghattas, J., Hauglustaine, D., Hu, R.-M., Kageyama, M., Khodri, M., Lebas, N., Levavasseur, G., Marchand, M., Ottlé, C., Peylin, P., Sima, A., Szopa, S., Thiéblemont, R., Vuichard, N., and Boucher O.: Implementation of the CMIP6 forcing data in the IPSL-CM6A-LR model, J. Adv. Model. Earth Sy., 12, e2019MS001940, https://doi.org/10.1029/2019MS001940, 2020.

Mann, G. W., Carslaw, K. S., Spracklen, D. V., Ridley, D. A., Manktelow, P. T., Chipperfield, M. P., Pickering, S. J., and Johnson, C. E.: Description and evaluation of GLOMAP-mode: a modal global aerosol microphysics model for the UKCA composition-climate model, Geosci. Model Dev., 3, 519–551, https://doi.org/10.5194/gmd-3-519-2010, 2010.

Mann, G. W., Carslaw, K. S., Ridley, D. A., Spracklen, D. V., Pringle, K. J., Merikanto, J., Korhonen, H., Schwarz, J. P., Lee, L. A., Manktelow, P. T., Woodhouse, M. T., Schmidt, A., Breider, T. J., Emmerson, K. M., Reddington, C. L., Chipperfield, M. P., and Pickering, S. J.: Intercomparison of modal and sectional aerosol microphysics representations within the same 3-D global chemical transport model, Atmos. Chem. Phys., 12, 4449–4476, https://doi.org/10.5194/acp-12-4449-2012, 2012.

Marchand, M., Keckhut, P., Lefebvre, S., Claud, C., Cugnet, D., Hauchecorne, A., Lefèvre, F., Lefebvre, M.-P., Jumelet, J., Lott, F., Hourdin, F., Thuillier, G., Poulain, V., Bossay, S., Lemennais, P., David, C., and Bekki, S.: Dynamical amplification of the stratospheric solar response simulated with the Chemistry-Climate Model LMDz-Reprobus, J. Atmos. Sol.-Terr. Phy., 75–76, 147–160, https://doi.org/10.1016/j.jastp.2011.11.008, 2012.

Millán, L., Santee, M. L., Lambert, A., Livesey, N. J., Werner, F., Schwartz, M. J., Pumphrey, H. C., Manney, G. L., Wang, Y., Su, H., Wu, L., Read, W. G., and Froidevaux, L.: The Hunga Tonga-Hunga Ha'apai Hydration of the Stratosphere, Geophys. Res. Lett., 49, e2022GL099381, https://doi.org/10.1029/2022GL099381, 2022.

Mills, M. J., Toon, O. B., Vaida, V., Hintze, P. E., Kjaergaard, H. G., Schofield, D. P., and Robinson, T. W.: Photolysis of sulfuric acid vapor by visible light as a source of the polar stratospheric CN layer, J. Geophys. Res., 110, D08201, https://doi.org/10.1029/2004JD005519, 2005.

Mills, M. J., Schmidt, A., Easter, R., Solomon, S., Kinnison, D. E., Ghan, S. J., Neely, R. R., Marsh, D. R., Conley, A., Bardeen, C. G., and Gettelman, A.: Global volcanic aerosol properties derived from emissions, 1990–2014, using CESM1(WACCM), J. Geophys. Res.-Atmos., 121, 2332–2348, https://doi.org/10.1002/2015JD024290, 2016.

Mills, M. J., Richter, J. H., Tilmes, S., Kravitz, B., MacMartin, D. G., Glanville, A. A., Tribbia, J. J., Lamarque, J.-F., Vitt, F., Schmidt, A., Gettelman, A., Hannay, C., Bacmeister, J. T., and Kinnison, D. E.: Radiative and chemical response to interactive stratospheric sulfate aerosols in fully coupled CESM1(WACCM), J. Geophys. Res.-Atmos., 122, 13061–13078, https://doi.org/10.1002/2017JD027006, 2017.

Molod, A., Takacs, L., Suarez, M., and Bacmeister, J.: Development of the GEOS-5 atmospheric general circulation model: evolution from MERRA to MERRA2, Geosci. Model Dev., 8, 1339–1356, https://doi.org/10.5194/gmd-8-1339-2015, 2015.

Morgenstern, O., Braesicke, P., O'Connor, F. M., Bushell, A. C., Johnson, C. E., Osprey, S. M., and Pyle, J. A.: Evaluation of the new UKCA climate-composition model – Part 1: The stratosphere, Geosci. Model Dev., 2, 43–57, https://doi.org/10.5194/gmd-2-43-2009, 2009.

Morgenstern, O., Hegglin, M. I., Rozanov, E., O'Connor, F. M., Abraham, N. L., Akiyoshi, H., Archibald, A. T., Bekki, S., Butchart, N., Chipperfield, M. P., Deushi, M., Dhomse, S. S., Garcia, R. R., Hardiman, S. C., Horowitz, L. W., Jöckel, P., Josse, B., Kinnison, D., Lin, M., Mancini, E., Manyin, M. E., Marchand, M., Marécal, V., Michou, M., Oman, L. D., Pitari, G., Plummer, D. A., Revell, L. E., Saint-Martin, D., Schofield, R., Stenke, A., Stone, K., Sudo, K., Tanaka, T. Y., Tilmes, S., Yamashita, Y., Yoshida, K., and Zeng, G.: Review of the global models used within phase 1 of the Chemistry–Climate Model Initiative (CCMI), Geosci. Model Dev., 10, 639–671, https://doi.org/10.5194/gmd-10-639-2017, 2017.

Mulcahy, J. P., Jones, C., Sellar, A., Johnson, B., Boutle, I. A., Jones, A., Andrews T., Rumbold, S. T., Mollard, J., Bellouin, N., Johnson, C. E., Williams, K. D., Grosvenor, D. P., and McCoy D. T.: Improved Aerosol Processes and Effective Radiative Forcing in HadGEM3 and UKESM1, J. Adv. Model. Earth Sy., 10, 2786–2805, https://doi.org/10.1029/2018MS001464, 2018.

Mulcahy, J. P., Johnson, C., Jones, C. G., Povey, A. C., Scott, C. E., Sellar, A., Turnock, S. T., Woodhouse, M. T., Abraham, N. L., Andrews, M. B., Bellouin, N., Browse, J., Carslaw, K. S., Dalvi, M., Folberth, G. A., Glover, M., Grosvenor, D. P., Hardacre, C.,

Hill, R., Johnson, B., Jones, A., Kipling, Z., Mann, G., Mollard, J., O'Connor, F. M., Palmiéri, J., Reddington, C., Rumbold, S. T., Richardson, M., Schutgens, N. A. J., Stier, P., Stringer, M., Tang, Y., Walton, J., Woodward, S., and Yool, A.: Description and evaluation of aerosol in UKESM1 and HadGEM3-GC3.1 CMIP6 historical simulations, Geosci. Model Dev., 13, 6383–6423, https://doi.org/10.5194/gmd-13-6383-2020, 2020.

Mulcahy, J. P., Jones, C. G., Rumbold, S. T., Kuhlbrodt, T., Dittus, A. J., Blockley, E. W., Yool, A., Walton, J., Hardacre, C., Andrews, T., Bodas-Salcedo, A., Stringer, M., de Mora, L., Harris, P., Hill, R., Kelley, D., Robertson, E., and Tang, Y.: UKESM1.1: development and evaluation of an updated configuration of the UK Earth System Model, Geosci. Model Dev., 16, 1569–1600, https://doi.org/10.5194/gmd-16-1569-2023, 2023.

Naujokat, B.: An update of the observed Quasi-Biennial Oscillation of the stratospheric winds over the tropics, J. Atmos. Sci., 43, 1873–1877, https://doi.org/10.1175/1520-0469(1986)043<1873:AUOTOQ>2.0.CO;2, 1986.

Neely III, R. R. and Schmidt, A.: VolcanEESM: Global volcanic sulphur dioxide (SO_2) emissions database from 1850 to present, Centre for Environmental Data Analysis [data set], https://doi.org/10.5285/76ebdc0b-0eed-4f70-b89e-55e606bcd568, 2016.

Nielsen, J. E., Pawson, S., Molod, A., Auer, B., Da Silva, A. M., Douglass, A. R., Duncan, B., Liang, Q., Manyin, M., Oman, L. D., Putman, W., Strahan, S., and Wargan, K.: Chemical mechanisms and their applications in the Goddard Earth Observing System (GEOS) earth system model, J. Adv. Model. Earth Sy., 9, 3019–3044, https://doi.org/10.1002/2017MS001011, 2017.

O'Connor, F. M., Johnson, C. E., Morgenstern, O., Abraham, N. L., Braesicke, P., Dalvi, M., Folberth, G. A., Sanderson, M. G., Telford, P. J., Voulgarakis, A., Young, P. J., Zeng, G., Collins, W. J., and Pyle, J. A.: Evaluation of the new UKCA climate-composition model – Part 2: The Troposphere, Geosci. Model Dev., 7, 41–91, https://doi.org/10.5194/gmd-7-41-2014, 2014.

O'Neill, B. C., Tebaldi, C., van Vuuren, D. P., Eyring, V., Friedlingstein, P., Hurtt, G., Knutti, R., Kriegler, E., Lamarque, J.-F., Lowe, J., Meehl, G. A., Moss, R., Riahi, K., and Sanderson, B. M.: The Scenario Model Intercomparison Project (ScenarioMIP) for CMIP6, Geosci. Model Dev., 9, 3461–3482, https://doi.org/10.5194/gmd-9-3461-2016, 2016.

Peuch, V.-H., Engelen, R., Rixen, M., Dee, D., Flemming, J., Suttie, M., Ades, M., Agusti-Panareda, A., Ananasso, C., Andersson, E., Armstrong, D., Barre, J., Bousserez, N., Dominguez, J. J., Garrigues, S., Inness, A., Jones, L., Kipling, Z., Letertre-Danczak, J., Parrington, M., Razinger, M., Ribas, R., Vermoote, S., Yang, X., Simmons, A., de Marcilla, J. G., and Thepaut, J.-N.: The Copernicus Atmosphere Monitoring Service: From Research to Operations, B. Am. Meteorol. Soc., 103, E2650–E2668, https://doi.org/10.1175/BAMS-D-21-0314.1, 2022.

Pringle, K. J., Tost, H., Message, S., Steil, B., Giannadaki, D., Nenes, A., Fountoukis, C., Stier, P., Vignati, E., and Lelieveld, J.: Description and evaluation of GMXe: a new aerosol submodel for global simulations (v1), Geosci. Model Dev., 3, 391–412, https://doi.org/10.5194/gmd-3-391-2010, 2010.

Putman, W. M. and Lin, S. J.: Finite-volume transport on various cubed-sphere grids, J. Comput. Phys., 227, 55–78, 2007.

Quaglia, I., Aquila, V., and Zhuo, Z.: HTHHMOC zonal average H_2O anomaly in June 2022 from multi-model data, Zenodo [data set], https://doi.org/10.5281/zenodo.14963276, 2025.

Randel, W. J., Wang, X., Starr, J., Garcia, R. R., and Kinnison, D.: Long-term temperature impacts of the Hunga volcanic eruption in the stratosphere and above, Geophys. Res. Lett., 51, e2024GL111500, https://doi.org/10.1029/2024GL111500, 2024.

Reinecker, M., Suarez, M., Todling, R., Bacmeister, J., Takacs, L., and Liu, H.: The GEOS-5 data assimilation system-documentation of versions 5.0. 1, 5.1.0, No. NASA Tech Rep TM-2007, 104606, 2008.

Rémy, S., Kipling, Z., Huijnen, V., Flemming, J., Nabat, P., Michou, M., Ades, M., Engelen, R., and Peuch, V.-H.: Description and evaluation of the tropospheric aerosol scheme in the Integrated Forecasting System (IFS-AER, cycle 47R1) of ECMWF, Geosci. Model Dev., 15, 4881–4912, https://doi.org/10.5194/gmd-15-4881-2022, 2022.

Reynolds, R. W., Rayner, N. A., Smith, T. M., Stokes, D. C., and Wang, W.: An Improved In Situ and Satellite SST Analysis for Climate, J. Climate, 15, 1609–1625, https://doi.org/10.1175/1520-0442(2002)015<1609:AIISAS>2.0.CO;2, 2002.

Schallock, J., Brühl, C., Bingen, C., Höpfner, M., Rieger, L., and Lelieveld, J.: Reconstructing volcanic radiative forcing since 1990, using a comprehensive emission inventory and spatially resolved sulfur injections from satellite data in a chemistry-climate model, Atmos. Chem. Phys., 23, 1169–1207, https://doi.org/10.5194/acp-23-1169-2023, 2023.

Scinocca, J. F.: An Accurate Spectral Non-Orographic Gravity Wave Parameterization for General Circulation Models, J. Atmos. Sci., 60, 667–682, https://doi.org/10.1175/1520-0469(2003)060<0667:AASNGW>2.0.CO;2, 2003.

Scinocca, J. F., McFarlane, N. A., Lazare, M., Li, J., and Plummer, D.: Technical Note: The CCCma third generation AGCM and its extension into the middle atmosphere, Atmos. Chem. Phys., 8, 7055–7074, https://doi.org/10.5194/acp-8-7055-2008, 2008.

Seddon, J., Stephens, A., Mizielinski, M. S., Vidale, P. L., and Roberts, M. J.: Technology to aid the analysis of large-volume multi-institute climate model output at a central analysis facility (PRIMAVERA Data Management Tool V2.10), Geosci. Model Dev., 16, 6689–6700, https://doi.org/10.5194/gmd-16-6689-2023, 2023.

Sekiya, T., Sudo, K., and Nagai, T.: Evolution of stratospheric sulfate aerosol from the 1991 Pinatubo eruption: Roles of aerosol microphysical processes, J. Geophys. Res.-Atmos., 121, 2911–2938, https://doi.org/10.1002/2015JD024313, 2016.

Sellar, A., J., Jones, C. G., Mulcahy, J., Tang, Y., Andrew Yool, Andy Wiltshire, Fiona M. O'Connor, Marc Stringer, Hill, R., Palmieri, J., Woodward, S., de Mora, L., Kuhlbrodt, T., Rumbold, S. T., Kelley, D. I., Ellis, R., Johnson, C. E., Walton, J., Abraham, N. L., Andrews, M. B., Andrews, T., Archibald, A. T., Berthou, S., Burke, E., Blockley, E., Carslaw, K., Dalvi, M., Edwards, J., Folberth, G. A., Gedney, N., Griffiths, P. T., Harper, A. B., Hendry, M. A., Hewitt, A. J., Johnson, B., Jones, A., Jones, C. D., Keeble, J., Liddicoat, S., Morgenstern, O., Parker, R. J., Predoi, V., Robertson, E., Siahaan, A., Smith, R. S., Swaminathan, R., Woodhouse, M. T., Zeng, G., and Zerroukat, M.: UKESM1: Description and Evaluation of the U.K.

Earth System Model, J. Adv. Mod. Earth Sy., 11, 4513–4558, https://doi.org/10.1029/2019MS001739, 2019.

Sellar, A., Walton, J., Jones, C. G., Wood, R., Abraham, N. L., Andrejczuk, M., Andrews, M. B., Andrews, T., Archibald, A. T., de Mora, L., Dyson, H., Elkington, M., Ellis, R., Florek, P., Good, P., Gohar, L., Haddad, S., Hardiman, S. C., Hogan, E., Iwi, A., Jones, C. D., Johnson, B., Kelley, D. I., Kettleborough, J., Knight, J. R., Köhler, M. O., Kuhlbrodt, T., Liddicoat, S., Linova-Pavlova, I., Mizielinski, M. S., Morgenstern, O., Mulcahy, J., Neininger, E., O'Connor, F. M., Petrie, R., Ridley, J., Rioual, J.-C., Roberts, M., Robertson, E., Rumbold, S., Seddon, J., Shepherd, H., Shim, S., Stephens, A., Teixiera, J. C., Tang, Y., Williams, J., Wiltshire, A., and Griffiths P. T.: Implementation of U.K. Earth System Models for CMIP6, J. Adv. Mod. Earth Sy., 12, e2019MS001946, https://doi.org/10.1029/2019MS001946, 2020.

Sellitto, P., Podglajen, A., Belhadji, R., Boichu, M., Carboni, E., Cuesta, J., Duchamp, C., Kloss, C., Siddans, R., Bègue, N., Blarel, L., Jegou, F., Khaykin, S., Renard J.-B., and Legras B.: The unexpected radiative impact of the Hunga Tonga eruption of 15th January 2022, Communications Earth & Environment, 3, 288, https://doi.org/10.1038/s43247-022-00618-z, 2022.

SPARC: SPARC CCMVal Report on the Evaluation of Chemistry-Climate Models, edited by: Eyring, V., Shepherd, T., and Waugh, D., SPARC Report No. 5, WCRP-30/2010, WMO/TD – No. 40, https://www.aparc-climate.org/publications/sparc-reports/sparc-report-no-5/ (last access: 21 August 2025), 2010.

Strahan, S. E., Duncan, B. N., and Hoor, P.: Observationally derived transport diagnostics for the lowermost stratosphere and their application to the GMI chemistry and transport model, Atmos. Chem. Phys., 7, 2435–2445, https://doi.org/10.5194/acp-7-2435-2007, 2007.

Sukhodolov, T., Egorova, T., Stenke, A., Ball, W. T., Brodowsky, C., Chiodo, G., Feinberg, A., Friedel, M., Karagodin-Doyennel, A., Peter, T., Sedlacek, J., Vattioni, S., and Rozanov, E.: Atmosphere–ocean–aerosol–chemistry–climate model SOCOLv4.0: description and evaluation, Geosci. Model Dev., 14, 5525–5560, https://doi.org/10.5194/gmd-14-5525-2021, 2021.

Taha, G., Loughman, R., Zhu, T., Thomason, L., Kar, J., Rieger, L., and Bourassa, A.: OMPS LP Version 2.0 multi-wavelength aerosol extinction coefficient retrieval algorithm, Atmos. Meas. Tech., 14, 1015–1036, https://doi.org/10.5194/amt-14-1015-2021, 2021.

Taha, G., Loughman, R., Colarco, P. R., Zhu, T., Thomason, L. W., and Jaross, G.: Tracking the 2022 Hunga Tonga-Hunga Ha'apai aerosol cloud in the upper and middle stratosphere using space-based observations, Geophys. Res. Lett., 49, e2022GL100091, https://doi.org/10.1029/2022GL100091, 2022.

Tatebe, H., Ogura, T., Nitta, T., Komuro, Y., Ogochi, K., Takemura, T., Sudo, K., Sekiguchi, M., Abe, M., Saito, F., Chikira, M., Watanabe, S., Mori, M., Hirota, N., Kawatani, Y., Mochizuki, T., Yoshimura, K., Takata, K., O'ishi, R., Yamazaki, D., Suzuki, T., Kurogi, M., Kataoka, T., Watanabe, M., and Kimoto, M.: Description and basic evaluation of simulated mean state, internal variability, and climate sensitivity in MIROC6, Geosci. Model Dev., 12, 2727–2765, https://doi.org/10.5194/gmd-12-2727-2019, 2019.

Telford, P. J., Braesicke, P., Morgenstern, O., and Pyle, J. A.: Technical Note: Description and assessment of a nudged version of the new dynamics Unified Model, Atmos. Chem. Phys., 8, 1701–1712, https://doi.org/10.5194/acp-8-1701-2008, 2008.

Telford, P., Braesicke, P., Morgenstern, O., and Pyle, J.: Reassessment of causes of ozone column variability following the eruption of Mount Pinatubo using a nudged CCM, Atmos. Chem. Phys., 9, 4251–4260, https://doi.org/10.5194/acp-9-4251-2009, 2009.

Thomason, L. W., Ernest, N., Millán, L., Rieger, L., Bourassa, A., Vernier, J.-P., Manney, G., Luo, B., Arfeuille, F., and Peter, T.: A global space-based stratospheric aerosol climatology: 1979–2016, Earth Syst. Sci. Data, 10, 469–492, https://doi.org/10.5194/essd-10-469-2018, 2018.

Tilmes, S., Mills, M. J., Zhu, Y., Bardeen, C. G., Vitt, F., Yu, P., Fillmore, D., Liu, X., Toon, B., and Deshler, T.: Description and performance of a sectional aerosol microphysical model in the Community Earth System Model (CESM2), Geosci. Model Dev., 16, 6087–6125, https://doi.org/10.5194/gmd-16-6087-2023, 2023.

Tsujino, H., Urakawa, S., Nakano, H., Small, R. J., Kim, W. M., Yeager, S. G., Danabasoglu, G., Suzuki, T., Bamber, J. L., Bentsen, M., Böning, C. W., Bozec, A., Chassignet, E. P., Curchitser, E., Dias, F. B., Durack, P. J., Griffies, S.M., Harada, Y., Ilicak, M., Josey, S. A., Kobayashi, C., Kobayashi, S., Komuro, Y., Large, W. G., Le Sommer, J., Marsland, S. J., Masina, S., Scheinert, M., Tomita, H., Valdivieso, M., and Yamazaki D.: JRA-55 based surface dataset for driving ocean–sea-ice models (JRA55-do), Ocean Model., 130, 79–139, 2018.

Vehkamäki, H., Kulmala, M., Napari, I., Lehtinen, K. E., Timmreck, C., Noppel, M., and Laaksonen, A.: An improved parameterization for sulfuric acid-water nucleation rates for tropospheric and stratospheric conditions, J. Geophys. Res.-Atmos., 107, AAC 3-1–AAC 3-10, https://doi.org/10.1029/2002JD002184, 2002.

Walters, D., Baran, A. J., Boutle, I., Brooks, M., Earnshaw, P., Edwards, J., Furtado, K., Hill, P., Lock, A., Manners, J., Morcrette, C., Mulcahy, J., Sanchez, C., Smith, C., Stratton, R., Tennant, W., Tomassini, L., Van Weverberg, K., Vosper, S., Willett, M., Browse, J., Bushell, A., Carslaw, K., Dalvi, M., Essery, R., Gedney, N., Hardiman, S., Johnson, B., Johnson, C., Jones, A., Jones, C., Mann, G., Milton, S., Rumbold, H., Sellar, A., Ujiie, M., Whitall, M., Williams, K., and Zerroukat, M.: The Met Office Unified Model Global Atmosphere 7.0/7.1 and JULES Global Land 7.0 configurations, Geosci. Model Dev., 12, 1909–1963, https://doi.org/10.5194/gmd-12-1909-2019, 2019.

Wang, X.: MLS H_2O anomaly 2022, Zenodo [data set], https://doi.org/10.5281/zenodo.14962954, 2025.

Wang, X., Randel, W., Zhu, Y., Tilmes, S., Starr, J., Yu, W., Garcia, R., Toon, O. B., Park, M., Kinnison, D., Zhang, J., Bourassa, A., Rieger, L., Warnock, T., and Li, J.: Stratospheric climate anomalies and ozone loss caused by the Hunga Tonga-Hunga Ha'apai volcanic eruption, J. Geophys. Res.-Atmos., 128, e2023JD039480, https://doi.org/10.1029/2023JD039480, 2023.

Watanabe, S., Hajima, T., Sudo, K., Nagashima, T., Takemura, T., Okajima, H., Nozawa, T., Kawase, H., Abe, M., Yokohata, T., Ise, T., Sato, H., Kato, E., Takata, K., Emori, S., and Kawamiya, M.: MIROC-ESM 2010: model description and basic results of CMIP5-20c3m experiments, Geosci. Model Dev., 4, 845–872, https://doi.org/10.5194/gmd-4-845-2011, 2011.

Williams, J. E., Huijnen, V., Bouarar, I., Meziane, M., Schreurs, T., Pelletier, S., Marécal, V., Josse, B., and Flemming, J.: Regional evaluation of the performance of the global CAMS chemical

modeling system over the United States (IFS cycle 47r1), Geosci. Model Dev., 15, 4657–4687, https://doi.org/10.5194/gmd-15-4657-2022, 2022.

Williams, K. D., Copsey, D., Blockley, E. W., Bodas-Salcedo, A., Calvert, D., Comer, R., Davis, P., Graham, T., Hewitt, H. T., Hill, R., Hyder, P., Ineson, S., Johns, T. C., Keen, A. B., Lee, R. W., Megann, A., Milton, S. F., Rae, J. G. L., Roberts, M. J., Scaife, A. A., Schiemann, R., Storkey, D., Thorpe, L., Watterson, I. G., Walters, D. N., West, A., Wood, R. A., Woollings, T., and Xavier, P. K.: The Met Office Global Coupled Model 3.0 and 3.1 (GC3.0 and GC3.1) Configurations, J. Adv. Model. Earth Sy., 10, 357–380, https://doi.org/10.1002/2017MS001115, 2018.

Wood, N., Staniforth, A., White, A., Allen, T., Diamantakis, M., Gross, M., Melvin, T., Smith, C., Vosper, S., Zerroukat, M., and Thuburn, J.: An inherently mass-conserving semi-implicit semi-Lagrangian discretization of the deep-atmosphere global nonhydrostatic equations, Q. J. Roy. Meteor. Soc., 140, 1505–1520, https://doi.org/10.1002/qj.2235, 2014.

Yu, P., Toon, O. B., Bardeen, C. G., Mills, M. J., Fan, T., English, J. M., and Neely, R. R.: Evaluations of tropospheric aerosol properties simulated by the community earth system model with a sectional aerosol microphysics scheme, J. Adv. Model. Earth Sy., 7, 865–914, https://doi.org/10.1002/2014MS000421, 2015.

Yu, W., Garcia, R., Yue, J., Smith, A., Wang, X., Randel, W., Qiao, Z., Zhu, Y., Harvey, V. L., Tilmes, S., and Mlynczak, M.: Mesospheric temperature and circulation response to the Hunga Tonga-Hunga-Ha‘apai volcanic eruption, J. Geophys. Res.-Atmos., 128, e2023JD039636, https://doi.org/10.1029/2023JD039636, 2023.

Zhang, J., Kinnison, D., Zhu, Y., Wang, X., Tilmes, S., Dube, K., and Randel, W.: Chemistry contribution to stratospheric ozone depletion after the unprecedented water-rich Hunga Tonga eruption, Geophys. Res. Lett., 51, e2023GL105762, https://doi.org/10.1029/2023GL105762, 2024.

Zhou, X., Dhomse, S. S., Feng, W., Mann, G., Heddell, S., Pumphrey, H., Kerridge, B. J., Latter, B., Siddans, R., Ventress, L., Querel, R., Smale, P., Asher, E., Hall, E. G., Bekki, S., and Chipperfield, M. P.: Antarctic vortex dehydration in 2023 as a substantial removal pathway for Hunga Tonga-Hunga Ha‘apai water vapor, Geophys. Res. Lett., 51, e2023GL107630, https://doi.org/10.1029/2023GL107630, 2024.

Zhu, Y., Bardeen, C. G., Tilmes, S., Mills, M. J., Wang, X., Harvey, V. L., Taha, G., Kinnison, D., Portmann, R. W., Yu, P., Rosenlof, K. H., Avery, M., Kloss, C., Li, C., Glanville, A. S., Millán, L., Deshler, T., Krotkov, N., and Toon O. B.: Perturbations in stratospheric aerosol evolution due to the water-rich plume of the 2022 Hunga-Tonga eruption, Commun. Earth Environ., 3, 248, https://doi.org/10.1038/s43247-022-00580-w, 2022.